Contemporary Mathematics
http://ojs.wiserpub.com/index.php/CM/

UNIVERSAL WISER PUBLISHER

Research Article

An Application of the Caputo Fractional Domain in the Analysis of a COVID-19 Mathematical Model

Chandrali Baishya[1], Sindhu J. Achar[2], P. Veeresha[3*]

[1]Department of Studies and Research in Mathematics, Tumkur University, Tumkur 572103, India
[2]Department of Mathematics and Statistics, M. S. Ramaiah University of Applied Sciences, Bangalore 560058, Karnataka, India
[3]Center for Mathematical Needs, Department of Mathematics, CHRIST (Deemed to be University), Bengaluru 560029, India
Email: pundikala.veeresha@christuniversity.in

Received: 18 January 2023; **Revised:** 23 February 2023; **Accepted:** 27 February 2023

Abstract: Vaccination programs aimed at preventing the spread of the coronavirus appear to have a significant global impact. In this research, we have investigated a mathematical model projecting COVID-19 disease spread by considering five groups of individuals viz. vulnerable, exposed, infected, unreported, recovered, and vaccinated. Looking at the current abnormal pattern of the virus spread in the projected model, we have implemented the fractional derivative in the Mittag-Leffler context. Using the existing theory of the fractional derivative, we have examined the theoretical aspects such as the existence and uniqueness of the solutions, the existence and stability of the disease-free and endemic equilibrium points, and the global stability of the disease-free equilibrium point. In computing the basic reproduction number, we have analyzed that the existence and stability of points of equilibrium are dependent on this number. The sensitivity of the basic reproduction number is also examined. The importance of the vaccination drive is highlighted by relating it to the basic reproduction number. Finally, we have presented the simulation of the numerical results by capturing the profile of each group under the influence of the fractional derivative and investigated the impact of vaccination rate and contact rate in controlling the disease by applying the Adams-Bashforth-Moultan (ABM) method. The present research study demonstrates the importance of the vaccination campaign and the curb on individual contact by featuring a novel fractional operator in the projected model and capturing the corresponding consequence.

***Keywords*:** susceptible-exposed-infectious-recovered (SEIR) model, COVID-19, vaccination, Caputo fractional derivative, ABM method

MSC: 34A34, 26A33, 92D30

1. Introduction

One of the greatest life-changing events of our time is the COVID-19 outbreak, which resulted from the SARS-CoV-2, a contemporary coronavirus. This virus, on the other hand, has a long history stretching back more than six decades. In 1965, the first human coronavirus was found. Later that decade, scientists found a collection of human and animal viruses that they dubbed "crown viruses" because of their crown-like appearance. Discovered in 2002 in southern China for the first time, SARS quickly spread to 28 other countries. Another class of coronavirus, first

DOI: https://doi.org/10.37256/cm.5120242363

discovered in Saudi Arabia in 2012, was the Middle East respiratory syndrome (MERS) [1]. While less infectious than SARS, the coronavirus is more deadly, having killed 858 people. It has the same respiratory symptoms as a common cold, but it also has the potential to cause kidney failure. On December 31, 2019, the World Health Organization (WHO) discovered a new strain of this virus, COVID-19, after analyzing a cluster of cases of "viral pneumonia" in Wuhan, People's Republic of China. According to scientists, SARS-CoV-2, believed to have emerged in bats, was discovered in one of Wuhan's open-air "wet markets" It causes colds, dry coughs, and breathing difficulties in people. Approximately, 15% become critically ill, needing intensive treatment, and 5% become severely ill, requiring oxygen. In rare cases, children can develop a severe inflammatory syndrome a few weeks after infection [2-4]. The spread of this illness has changed the livelihood of humankind. Two years ago, none of us would have predicted that masks, social distancing, working from home, and online education would become a part of our daily lives. However, this seems to be the new standard. The virus that causes COVID-19, SARS-CoV-2, develops like all viruses. When a virus replicates or repeats itself, it may change significantly, as viruses do. Mutations are the scientific term for these changes. When a virus is widely dispersed in a population and causes repeated illnesses, its risk of mutation increases. As the COVID-19 epidemic sweeps the globe, WHO and its partners are scrambling to find and deploy safe and effective vaccinations. The vaccine is a crucial new weapon in the fight against COVID-19, and the very encouraging fact is that so many are being produced and have been demonstrated to be effective. Scientists from all across the world are scrambling to develop studies, treatments, and vaccines that will save lives and bring the pandemic to an end as soon as possible. As of February 18, 2021, at least seven different vaccines, including Sputnik V, Covishield, Covaxin, Pfizer-BioNTech, Johnson & Johnson's Janssen, Moderna, and others, had been tested in countries across three networks [5-7]. Vaccination for vulnerable populations is prioritized in all countries. At the same time, more than 200 other vaccine candidates are being developed, but only 60 of them are now in clinical trials [8, 9]. Safe and efficient vaccination is the only way to eradicate this pandemic from the world. As per the WHO report as of April 21, 2021, among the world's total population of 7,845,261,000, the COVID-19 infection data is listed as follows: confirmed cases: 143,123,631, total deaths: 3,045,018, total recovery cases: 82,117,879; total population vaccinated: 207,978,809 [5]. Whereas as of September 24, 2021, around the world, including 4,724,876 deaths, there had been 230,418,451 confirmed cases of COVID-19. A total of 5,874,934,542 vaccine doses have been provided as of September 22, 2021 [5]. We can clearly notice the rapid vaccination drive within a span of five months.

Although fractional differentiation is 323 years old, the notion has received a lot of attention and consideration in the last 55 years, specifically in 1967, when it was first modified as part of the Caputo investigation [10]. In recent years, we have noticed rigorous applications of fractional calculus in various fields to model numerous real-world phenomena [11]. Significant literature on these works can be found in [12-14]. Over the decades, Riemann-Liouville and Caputo fractional derivative (FD) received special attention from the research community. The Caputo FD has the advantage of allowing standard initial conditions to be incorporated into the model formulation [10]. Additionally, the derivative of a constant is zero under the Caputo FD. Although these FDs provide a lot of benefits, they aren't appropriate for every case. The exponential functions are the eigenfunctions of the decay differential ordinary equations and also the generator of an evolution partial differential equation with a classical derivative [15].

The study of disease dynamics has remained one of the most popular themes for many scientific communities. Evolution in the area of fractional calculus has appeared as an added advantage in this process [16-24]. The Caputo, Riemann-Liouville, Grünwald Letnikov, and Jumarie fractional operators are a few among the FDs that have gained importance among researchers in evaluating disease dynamics. In [16, 17], authors have analyzed the dynamics of a fractional epidemiological model and obtained remarkable results. An interesting application of the fractional epidemic model is presented in [19], where the authors have applied it to a pest management system. A numerical analysis of the fractional order model of HIV-1 infection of CD4+ T-cells is performed in [20]. New numerical methods to solve fractional differential equations are presented in [21, 22]. Apart from these derivatives, the Atangana-Baleanu derivative [25, 26] is one of the derivatives that is attracting researchers to evaluate epidemiology. Applying Caputo-Fabrizio FD to the epidemiological model, many remarkable works have been delivered by researchers [27, 28]. In the works of Baleanu et al. [29], Kojabad et al. [30], and Qureshi et al. [31], fractional extensions of integer-order mathematical models have been proven to be more systematic while representing the natural facts about disease dynamics. At the time of the outbreak of novel coronaviruses, mathematicians have continuously worked on modeling and have come up with many effective mathematical models of integer and fractional order to simulate the transmission of coronaviruses [32-

43]. In [35], authors have fitted a fractional stochastic model to study the COVID-19 spread in Egypt. In [38], authors have applied the fractional COVID-19 model to study the SARS transmission in China. Safare et al. [42] have applied nonsingular FD to analyze COVID-19 spread. Vellappandi et al. [43] have studied COVID-19 spread in Russia.

The effect of hysteresis is introduced to the biological model by [44] because certain live organisms' defense mechanisms are triggered by it. The FD is a generalization of the integer-order derivative that has been demonstrated to be more effective in replicating real-world problems involving memory effects. The FDs are significant in analyzing the hysteresis effect since the past is seen as the source of the present. In [45, 46], the theory of fractional calculus is employed to examine the epidemic's evolution. Previous experiences suggest that, during a disease like COVID-19, hygiene habits or social distance are defensive actions to limit the transmission of an infectious disease in humans. When a vaccine has a long-term memory impact, it causes the body to defend itself through immunological memory. As a result, employing classical differential equations to model the dynamics of the populations involved may be ineffective. FDs' ability to capture heterogeneous and memory-based properties motivated us to incorporate fractional operators in the projected COVID-19 model. The main objective of this study is to observe the influence of memory impact in terms of social contact, vaccination, etc. on the spread and control of COVID-19. In this paper, we look at the impact of hysteresis on disease propagation by considering the effects of all prior states on present dynamical stages with the incorporation of the Caputo operator. We explore the evolution of COVID-19 in a population to demonstrate the potential of fractional differential equations in epidemiological processes. Whenever any virus infection erupts in the population, it never disappears completely. In some corners of the planet, a small number of individuals remain infected by this disease. This phenomenon of coexistence can be very well depicted by fractional calculus. In this connection, we use the Caputo fractional-order derivative to investigate the COVID-19 transmission model. As the COVID-19 vaccines are launched all over the world, we intend to incorporate vaccination terms in the model and examine the numerical simulation of COVID-19 spread and the impact of vaccination on it. The influence of vaccination in controlling the disease is projected by computing the basic reproduction (BR) number. Since one of the measures to be taken in managing epidemics is to restrict contact among the population, we have investigated the role of contact rate in controlling the spread. Connecting the impact of vaccination with the BR number and analyzing the sensitivity of the BR number concerning the parameters is the specific contribution of this work. The numerical results obtained using the fractional Adams-Bashforth-Moultan (ABM) method are compatible with the Caputo FD [47-51].

2. Preliminaries

Here, we have used the Caputo FDs because they support the integer-order initial condition. In this section, we have presented certain theorems that have been applied to determine the theoretical results corresponding to the solution of the projected model.

Definition 2.1. [13] Suppose $g(\mathrm{t})$ is k times continuously differentiable function. The FD of the order α for $g(t)$ in the Caputo sense is

$$D_{\mathrm{t}}^{\alpha} g(\mathrm{t}) = \frac{1}{\Gamma(k-\alpha)} \int_{\mathrm{t}_0}^{\mathrm{t}} \frac{g^{(k)}(\tau)}{(\mathrm{t}-\tau)^{\alpha+1-k}} d\tau, \tag{1}$$

where $\Gamma(\cdot)$ refers to gamma function, $\mathrm{t} > a$ and k is a positive integer with the property that $k-1 < \alpha < k$.

Lemma 2.2. [13] Consider the system

$$D_{\mathrm{t}}^{\alpha} v(\mathrm{t}) = g(\mathrm{t}, v), \mathrm{t} > \mathrm{t}_0, \tag{2}$$

choosing the initial condition as $v(\mathrm{t}_0)$, where $0 < \alpha \leq 1$ and $g : [\mathrm{t}_0, \infty) \times \Omega \to \mathbb{R}^n, \Omega \in \mathbb{R}^n$. When $g(\mathrm{t}, v)$ holds the locally Lipchitz conditions concerning v, equation (2) has a unique solution on $[\mathrm{t}_0, \infty) \times \Omega$.

Lemma 2.3. [52] We assume that $g(\mathrm{t})$ is a continuous function on $[\mathrm{t}_0, +\infty)$ satisfying

$$D_{\mathrm{t}}^{\alpha} g(\mathrm{t}) \leq -\epsilon g(\mathrm{t}) + \xi, g(\mathrm{t}_0) = g_0,$$

where $t_0 \geq 0$ is the initial time, $0 < \alpha \leq 1, \epsilon \neq 0$, $(\epsilon, \xi) \in \mathbb{R}^2$. Then,

$$g(t) \leq (g(t_0) - \frac{\xi}{\epsilon}) E_\alpha[-\epsilon(t - t_0)^\alpha] + \frac{\xi}{\epsilon}. \tag{3}$$

3. Model formulation

Mathematical modeling is regarded as a crucial tool for analyzing epidemic models and forecasting their futures by capturing their effects. The well-known susceptible-exposed-infectious-recovered (SEIR) model is used to illustrate the evolution of the fatal coronavirus in this study. Observing the present nature of infection among people, we have incorporated the unreported cases into the model. As vaccination is launched in various countries, seeking a more realistic model, we have included the equation representing the evolution of vaccination [53-55]. In the model formulation, we denote the total global human population size by $N(t)$, which is classified further into five classes: exposed $E(t)$, susceptible $S(t)$, unreported $U(t)$, infected $I(t)$, and recovered $R(t)$, at any time t, so that $N(t) = S(t) + E(t) + I(t) + U(t) + R(t)$. The vaccinated people are considered to be a non-vulnerable group of individuals and are denoted by $V(t)$. The schematic diagram of the interaction is projected in Figure 1. The arrows indicate the amount of population moving from one category to another. It can be seen from the figure that a portion of the exposed population moves to the infected group, whereas the remaining portion remains unreported. The biological meaning of the parameters is mentioned in Table 1.

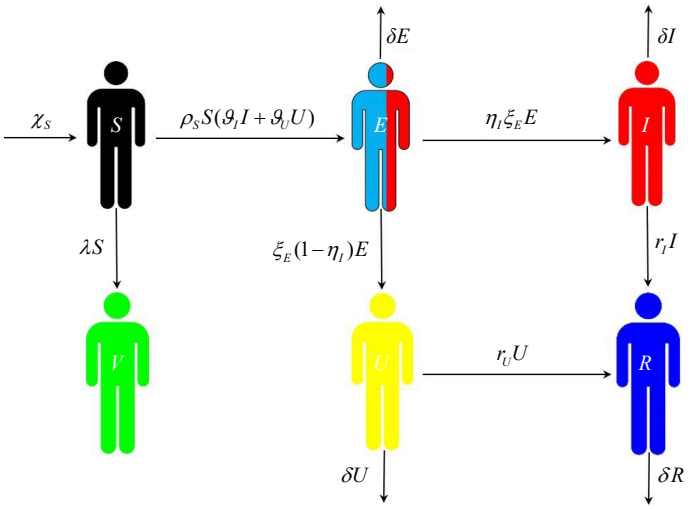

Figure 1. Schematic diagram of interaction among various groups of population

Table 1. Meaning of the symbols used in system (4)

χ_S	$n \times N$, n is the birth rate and N is the total population of world
ρ_S	Contact rate
ϑ_I	Disease transmission rate from I
ϑ_U	Disease transmission rate from U
λS	Vaccination rate
ξ_E	Rate of exposed population being infected
δ	Natural death rate of humans
η_I	Rate at which E progresses to I
r_I	Recovery rate of infected population
r_U	Recovery rate of unreported population

The assumptions of the projected COVID-19 model can be stated below:

1. Susceptible when contacted either by an infected or unreported group, they are exposed to the disease and, at the rate of $\nu S(\phi_1 + \phi_2)(I+U)$, move to the exposed compartment.
2. Exposed population joins the infected compartment at the rate of $\eta_I \xi_E E$ and the unreported compartment at the rate of $\xi_E(1-\eta_I)E$.
3. Both the infected and unreported populations join the recovery compartment at the rate of $r_I I$ and $r_U US$, respectively.
4. Susceptible population gets vaccinated at the rate of λS.

Based on the above assumptions, the interaction among these populations is presented through the following fractional evolutionary differential equations in the Caputo sense:

$$\begin{aligned} D_t^\alpha S &= \chi_S - \rho_S S(\vartheta_I I + \vartheta_U U) - \lambda S, \\ D_t^\alpha E &= \rho_S S(\vartheta_I I + \vartheta_U U) - \xi_E E - \delta E, \\ D_t^\alpha I &= \eta_I \xi_E E - r_I I - \delta I, \\ D_t^\alpha U &= \xi_E(1-\eta_I)E - r_U U - \delta U, \\ D_t^\alpha R &= r_I I + r_U U - \delta R, \\ D_t^\alpha V &= \lambda S, \end{aligned} \tag{4}$$

with $S(t) > 0$, $E(t) > 0$, $I(t) > 0$, $U(t) > 0$, $R(t) > 0$ and $V(t) > 0$, and where t_0 is the initial time. All the parameters $\chi_S, \rho_S, \vartheta_I, \vartheta_U, \lambda, \xi_E, \delta, \eta_I, r_I$, and r_U are positive.

4. Existence of solutions

The existence, and uniqueness of the solutions of the proposed model (4) are established using the Banach fixed point theorem in this section. Even though there are no direct approaches for evaluating the exact solutions of the model due to its complexity and non-local behavior, the existence of the solution can be assured if certain conditions are met. Then, by (4)

$$
\begin{aligned}
D_t^{\alpha}[S(t)] &= \mathcal{G}_1(t,S),\\
D_t^{\alpha}[E(t)] &= \mathcal{G}_2(t,E),\\
D_t^{\alpha}[I(t)] &= \mathcal{G}_3(t,I),\\
D_t^{\alpha}[U(t)] &= \mathcal{G}_4(t,U),\\
D_t^{\alpha}[R(t)] &= \mathcal{G}_5(t,R),\\
D_t^{\alpha}[V(t)] &= \mathcal{G}_6(t,V).
\end{aligned} \tag{5}
$$

With Volterra type integral equation, we have

$$
\begin{aligned}
S(t)-S(t_0) &= \frac{1}{\Gamma(\alpha)}\int_{t_0}^{t}\mathcal{G}_1(\vartheta,S)(t-\vartheta)^{\alpha-1}d\vartheta,\\
E(t)-E(t_0) &= \frac{1}{\Gamma(\alpha)}\int_{t_0}^{t}\mathcal{G}_2(\vartheta,E)(t-\vartheta)^{\alpha-1}d\vartheta,\\
I(t)-I(t_0) &= \frac{1}{\Gamma(\alpha)}\int_{t_0}^{t}\mathcal{G}_3(\vartheta,I)(t-\vartheta)^{\alpha-1}d\vartheta,\\
U(t)-U(t_0) &= \frac{1}{\Gamma(\alpha)}\int_{t_0}^{t}\mathcal{G}_4(\vartheta,U)(t-\vartheta)^{\alpha-1}d\vartheta,\\
R(t)-R(t_0) &= \frac{1}{\Gamma(\alpha)}\int_{t_0}^{t}\mathcal{G}_5(\vartheta,R)(t-\vartheta)^{\alpha-1}d\vartheta,\\
V(t)-V(t_0) &= \frac{1}{\Gamma(\alpha)}\int_{t_0}^{t}\mathcal{G}_6(\vartheta,V)(t-\vartheta)^{\alpha-1}d\vartheta.
\end{aligned} \tag{6}
$$

Theorem 4.1. The kernel G_1 holds the Lipschitz condition and contraction if $0 \le (\rho_S(\vartheta_I\epsilon_3 + \vartheta_U\epsilon_4) + \lambda) < 1$ holds true.

Proof. We shall consider the two functions S and S_1 such as:

$$
\begin{aligned}
\| \mathcal{G}_1(t,S) - \mathcal{G}_1(t,S_1) \| &= \| \chi_S - \rho_S S(t)(\vartheta_I I(t) + \vartheta_U U(t)) - \lambda S(t) - \chi_S - \rho_S S(t_1)(\vartheta_I I(t) + \vartheta_U U(t)) - \lambda S(t_1) \|\\
&= \| \rho_S(\vartheta_I I(t) + \vartheta_U U(t))[S(t) - S(t_1)] - \lambda[S(t) - S(t_1)] \|\\
&\le (\rho_S(\vartheta_I \| I(t) \| + \vartheta_U \| U(t) \|) + \lambda) \| S(t) - S(t_1) \|\\
&\le (\rho_S\vartheta_I\epsilon_3 + \rho_S\vartheta_U\epsilon_4 + \lambda) \| S(t) - S(t_1) \|\\
&= \zeta_1 \| S(t) - S(t_1) \|.
\end{aligned} \tag{7}
$$

Taking $\zeta_1 = \rho_S\vartheta_I\epsilon_3 + \rho_S\vartheta_U\epsilon_4 + \lambda,$ where $\| I(t) \| \le \epsilon_3$ and $\| U(t) \| \le \epsilon_4$ are bounded functions, implies that

$$
\| \mathcal{G}_1(t,S) - \mathcal{G}_1(t,S_1) \| \le \zeta_1 \| S(t) - S(t_1) \|. \tag{8}
$$

We have $\| S(t) \| \le \epsilon_1, \| E(t) \| \le \epsilon_2, \| I(t) \| \le \epsilon_3, \| U(t) \| \le \epsilon_4, \| R(t) \| \le \epsilon_5,$ and $\| V(t) \| \le \epsilon_6$ are bounded functions and therefore, the Lipschitz condition is satisfied for G_1 and if $0 \le \rho_S\vartheta_I\epsilon_3 + \rho_S\vartheta_U\epsilon_4 + \lambda < 1,$ then it follows a contraction. Similarly, for the remaining cases it can be proved and represented as follows:

$$
\begin{aligned}
\| \mathcal{G}_2(t,E) - \mathcal{G}_2(t,E_1) \| &\le \zeta_2 \| E(t) - E(t_1) \|,\\
\| \mathcal{G}_3(t,I) - \mathcal{G}_3(t,I_1) \| &\le \zeta_3 \| I(t) - I(t_1) \|,\\
\| \mathcal{G}_4(t,U) - \mathcal{G}_4(t,U_1) \| &\le \zeta_4 \| U(t) - U(t_1) \|,\\
\| \mathcal{G}_5(t,R) - \mathcal{G}_5(t,R_1) \| &\le \zeta_5 \| R(t) - R(t_1) \|,\\
\| \mathcal{G}_6(t,V) - \mathcal{G}_6(t,V_1) \| &\le \zeta_6 \| V(t) - V(t_1) \|.
\end{aligned} \tag{9}
$$

Now, by system (6), the recursive form can be written as

$$
\begin{aligned}
S_n(t) &= S_0(t) + \frac{1}{\Gamma(\alpha)}\int_{t_0}^{t} \mathcal{G}_1(\vartheta, S_{n-1})(t-\vartheta)^{\alpha-1} d\vartheta,\\
E_n(t) &= E_0(t) + \frac{1}{\Gamma(\alpha)}\int_{t_0}^{t} \mathcal{G}_2(\vartheta, E_{n-1})(t-\vartheta)^{\alpha-1} d\vartheta,\\
I_n(t) &= I_0(t) + \frac{1}{\Gamma(\alpha)}\int_{t_0}^{t} \mathcal{G}_3(\vartheta, I_{n-1})(t-\vartheta)^{\alpha-1} d\vartheta,\\
U_n(t) &= U_0(t) + \frac{1}{\Gamma(\alpha)}\int_{t_0}^{t} \mathcal{G}_4(\vartheta, U_{n-1})(t-\vartheta)^{\alpha-1} d\vartheta,\\
R_n(t) &= R_0(t) + \frac{1}{\Gamma(\alpha)}\int_{t_0}^{t} \mathcal{G}_5(\vartheta, R_{n-1})(t-\vartheta)^{\alpha-1} d\vartheta,\\
V_n(t) &= V_0(t) + \frac{1}{\Gamma(\alpha)}\int_{t_0}^{t} \mathcal{G}_6(\vartheta, V_{n-1})(t-\vartheta)^{\alpha-1} d\vartheta,
\end{aligned} \tag{10}
$$

with

$$
S_0(t) = S(t_0), E_0(t) = E(t_0), I_0(t) = I(t_0), U_0(t) = U(t_0), R_0(t) = R(t_0), V_0(t) = V(t_0).
$$

Then, by the successive terms difference, we have

$$
\begin{aligned}
\aleph_{1,n}(t) &= S_n(t) - S_{n-1}(t) = \frac{1}{\Gamma(\alpha)}\int_{t_0}^{t} (\mathcal{G}_1(\vartheta, S_{n-1}) - \mathcal{G}_1(\vartheta, S_{n-2}))(t-\vartheta)^{\alpha-1} d\vartheta,\\
\aleph_{2,n}(t) &= E_n(t) - E_{n-1}(t) = \frac{1}{\Gamma(\alpha)}\int_{t_0}^{t} (\mathcal{G}_2(\vartheta, E_{n-1}) - \mathcal{G}_2(\vartheta, E_{n-2}))(t-\vartheta)^{\alpha-1} d\vartheta,\\
\aleph_{3,n}(t) &= I_n(t) - I_{n-1}(t) = \frac{1}{\Gamma(\alpha)}\int_{t_0}^{t} (\mathcal{G}_3(\vartheta, I_{n-1}) - \mathcal{G}_3(\vartheta, I_{n-2}))(t-\vartheta)^{\alpha-1} d\vartheta,\\
\aleph_{4,n}(t) &= U_n(t) - U_{n-1}(t) = \frac{1}{\Gamma(\alpha)}\int_{t_0}^{t} (\mathcal{G}_4(\vartheta, U_{n-1}) - \mathcal{G}_4(\vartheta, U_{n-2}))(t-\vartheta)^{\alpha-1} d\vartheta,\\
\aleph_{5,n}(t) &= R_n(t) - R_{n-1}(t) = \frac{1}{\Gamma(\alpha)}\int_{t_0}^{t} (\mathcal{G}_5(\vartheta, R_{n-1}) - \mathcal{G}_5(\vartheta, R_{n-2}))(t-\vartheta)^{\alpha-1} d\vartheta,\\
\aleph_{6,n}(t) &= V_n(t) - V_{n-1}(t) = \frac{1}{\Gamma(\alpha)}\int_{t_0}^{t} (\mathcal{G}_6(\vartheta, V_{n-1}) - \mathcal{G}_6(\vartheta, V_{n-2}))(t-\vartheta)^{\alpha-1} d\vartheta.
\end{aligned} \tag{11}
$$

Notice that,

$$
\begin{aligned}
S_n(t) &= \sum_{i=1}^{n} \aleph_{1,i}(t),\\
E_n(t) &= \sum_{i=1}^{n} \aleph_{2,i}(t),\\
I_n(t) &= \sum_{i=1}^{n} \aleph_{3,i}(t),\\
U_n(t) &= \sum_{i=1}^{n} \aleph_{4,i}(t),\\
R_n(t) &= \sum_{i=1}^{n} \aleph_{5,i}(t),\\
V_n(t) &= \sum_{i=1}^{n} \aleph_{6,i}(t).
\end{aligned}
$$

By applying norm on system (11) and then using equation (8), we have

$$\| \aleph_{1,n}(t) \| \leq \frac{1}{\Gamma(\alpha)} \zeta_1 \int_{t_0}^{t} \left\| \aleph_{1,n-1}(\vartheta) \right\| d\vartheta,$$

$$\| \aleph_{2,n}(t) \| \leq \frac{1}{\Gamma(\alpha)} \zeta_2 \int_{t_0}^{t} \left\| \aleph_{2,n-1}(\vartheta) \right\| d\vartheta$$

$$\| \aleph_{3,n}(t) \| \leq \frac{1}{\Gamma(\alpha)} \zeta_3 \int_{t_0}^{t} \left\| \aleph_{3,n-1}(\vartheta) \right\| d\vartheta,$$

$$\| \aleph_{4,n}(t) \| \leq \frac{1}{\Gamma(\alpha)} \zeta_4 \int_{t_0}^{t} \left\| \aleph_{4,n-1}(\vartheta) \right\| d\vartheta,$$

$$\| \aleph_{5,n}(t) \| \leq \frac{1}{\Gamma(\alpha)} \zeta_5 \int_{t_0}^{t} \left\| \aleph_{5,n-1}(\vartheta) \right\| d\vartheta,$$

$$\| \aleph_{6,n}(t) \| \leq \frac{1}{\Gamma(\alpha)} \zeta_6 \int_{t_0}^{t} \left\| \aleph_{6,n-1}(\vartheta) \right\| d\vartheta. \tag{12}$$

By using the above theorem, we prove the following results.

Theorem 4.2. The solution of the system of fractional differential equations (4) will exist and is unique, if we obtain some t_0, such that

$$\frac{1}{\Gamma(\alpha)} \zeta_i t_0 < 1, \text{ for } i = 1, 2, 3, ..., 6.$$

Proof. Let $S(t)$, $E(t)$, $I(t)$, $U(t)$, $R(t)$, and $V(t)$ be the bounded functions, which satisfy the Lipschitz condition. Now, by equation (12), we have

$$\| \aleph_{1,i}(t) \| \leq \| S_n(t_0) \| \left[\frac{1}{\Gamma(\alpha)} \zeta_1 \right]^n,$$

$$\| \aleph_{2,i}(t) \| \leq \| E_n(t_0) \| \left[\frac{1}{\Gamma(\alpha)} \zeta_2 \right]^n,$$

$$\| \aleph_{3,i}(t) \| \leq \| I_n(t_0) \| \left[\frac{1}{\Gamma(\alpha)} \zeta_3 \right]^n,$$

$$\| \aleph_{4,i}(t) \| \leq \| U_n(t_0) \| \left[\frac{1}{\Gamma(\alpha)} \zeta_4 \right]^n,$$

$$\| \aleph_{5,i}(t) \| \leq \| R_n(t_0) \| \left[\frac{1}{\Gamma(\alpha)} \zeta_5 \right]^n,$$

$$\| \aleph_{6,i}(t) \| \leq \| V_n(t_0) \| \left[\frac{1}{\Gamma(\alpha)} \zeta_6 \right]^n. \tag{13}$$

Hence, both the existence and continuity are shown for the obtained solutions. To prove that the relation (13) is the solution for (4), we consider:

$$S(t) - S(t_0) = S_n(t) - \mathfrak{W}_{1n}(t),$$

$$E(t) - E(t_0) = E_n(t) - \mathfrak{W}_{2n}(t),$$

$$I(t) - I(t_0) = I_n(t) - \mathfrak{W}_{3n}(t),$$

$$U(t) - U(t_0) = U_n(t) - \mathfrak{W}_{4n}(t),$$

$$R(t) - R(t_0) = R_n(t) - \mathfrak{W}_{5n}(t),$$

$$V(t) - V(t_0) = V_n(t) - \mathfrak{W}_{6n}(t).$$

Now, we set

$$\begin{aligned}\|\mathfrak{W}_{1n}(t)\| &= \left\|\frac{1}{\Gamma(\alpha)}\int_{t_0}^{t}(t-\vartheta)^{\alpha-1}(\mathcal{G}_1(\vartheta,S)-\mathcal{G}_1(\vartheta,S_{n-1}))d\vartheta\right\| \\ &\leq \frac{1}{\Gamma(\alpha)}\int_{t_0}^{t}(t-\vartheta)^{\alpha-1}\left\|(\mathcal{G}_1(\vartheta,S)-\mathcal{G}_1(\vartheta,S_{n-1}))\right\|d\vartheta \\ &\leq \frac{1}{\Gamma(\alpha)}\zeta_1\left\|S-S_{n-1}\right\|t. \end{aligned} \tag{14}$$

Continuing the same procedure, at t_0, we get

$$\|\mathfrak{W}_{1n}(t)\| \leq \left(\frac{t_0}{\Gamma(\alpha)}\right)^{n+1}\zeta_1^{n+1}M. \tag{15}$$

From equation (15), we can see that as n tends to $\infty, \|\mathfrak{W}_{1n}(t)\|$ approach to 0 provided $\frac{t_0}{\Gamma(\alpha)}<1$. Similarly, it can be proved that all $\|\mathfrak{W}_{2n}(t)\|, \|\mathfrak{W}_{3n}(t)\|, \|\mathfrak{W}_{4n}(t)\|, \|\mathfrak{W}_{5n}(t)\|, \|\mathfrak{W}_{6n}(t)\|$ tends to 0. We prove uniqueness on contrary, if there exists other set of solutions $S^*(t)$, $E^*(t)$, $I^*(t)$, $U^*(t)$, $R^*(t)$, and $V^*(t)$.

Then,

$$S(t)-S^*(t)=\frac{1}{\Gamma(\alpha)}\int_{t_0}^{t}(\mathcal{G}_1(\vartheta,S)-\mathcal{G}_1(\vartheta,S^*))d\vartheta.$$

By employing the norm, the above equation becomes

$$\begin{aligned}\|S(t)-S^*(t)\| &= \|\frac{1}{\Gamma(\alpha)}\int_{t_0}^{t}(\mathcal{G}_1(\vartheta,S)-\mathcal{G}_1(\vartheta,S^*))d\vartheta\| \\ &\leq \frac{1}{\Gamma(\alpha)}\zeta_1 t\|S(t)-S^*(t)\|. \end{aligned} \tag{16}$$

On simplification

$$\left\|S(t)-S^*(t)\right\|\left(1-\frac{1}{\Gamma(\alpha)}\zeta_1 t_0\right)\leq 0.$$

Since

$$\left(1-\frac{1}{\Gamma(\alpha)}\zeta_1 t\right)\geq 0, \tag{17}$$

from the above inequality, it is clear that $S(t)-S^*(t)=0$. Hence, the equation (17) proves the required result.

5. Equilibrium analysis

In this section, we analyze the disease-free equilibrium and endemic equilibrium states of the system (4). Since the sixth equation of system (4) is a part of the susceptible population, we have not considered this equation of system (4) when computing the equilibrium point. The BR number and its sensitivity are examined. To find the points of equilibrium, from equation (4), we consider

$$\begin{aligned}
&\chi_S - \rho_S S(\vartheta_I I + \vartheta_U U) - \lambda S = 0,\\
&\rho_S S(\vartheta_I I + \vartheta_U U) - \xi_E E - \delta E = 0,\\
&\eta_I \xi_E E - r_I I - \delta I = 0,\\
&\xi_E (1-\eta_I) E - r_U U - \delta U = 0,\\
&r_I I + r_U U - \delta R = 0.
\end{aligned} \tag{18}$$

If all the eigenvalues $\Theta_i, i = 1, 2, ..., \beta$ of the Jacobian matrix $J(E)$, E being the point of equilibrium, satisfy the condition

$$|arg(eig(J(E)))| \;=\; |arg(\Theta_i)| > \frac{\alpha\pi}{2}, i = 1, 2, ..., \beta, \tag{19}$$

then the E is a stable point of equilibrium. To evaluate the eigenvalues, we solve the characteristic equation $|J(E) - \Theta_i I| = 0$.

Lemma 5.1. [56] Define the following characteristic equation

$$P(\Theta) = \Theta^{\beta} + A_1\Theta^{\beta-1} + A_2\Theta^{\beta-2} + ... + A_{\beta} = 0. \tag{20}$$

All the roots of the characteristic equation (20) satisfy the equation (19) if

1. For $\beta = 1$, the condition is $A_1 > 0$.
2. For $\beta = 2$, the conditions are $A_1 > 0$, $4A_2 > A_1^2$, $|\tan^{-1}\frac{\sqrt{4A_2 - A_1^2}}{A_1}| > \frac{\alpha\pi}{2}$.
3. For $\beta = 3$, if the discriminant of the polynomial $P(\Theta)$ is positive, then necessary and sufficient conditions to satisfy the equation (19) are

   $$A_1 > 0, A_2 > 0, A_1A_2 > A_3.$$

   If the discriminant of the polynomial $P(\Theta)$ is negative, then necessary and sufficient conditions to satisfy the equation (19) are

   $$A_1 > 0, A_2 > 0, A_1A_2 = A_3.$$

4. For general β, $A_{\beta} > 0$ is the necessary condition for equation (19) to be satisfied.

5.1 *BR number*

On solving the system (18), we obtain the disease-free equilibrium (DFE) point $E_0 = (\overline{S}, 0, 0, 0, 0) = (\frac{\chi_s}{\lambda}, 0, 0, 0, 0)$. DFE point is $E_0 = (\frac{\chi_S}{\lambda}, 0, 0, 0, 0)$. We compute the BR number by evaluating the next-generation matrix. To compute BR number R_0, we consider

$$D_t^{\alpha}(\Delta(t)) = F(t) - V(t), \tag{21}$$

where

$$F(t) = \begin{pmatrix} S\rho_S\left(I\vartheta_I + U\vartheta_U\right) \\ 0 \\ 0 \end{pmatrix} \text{ and } V(t) = \begin{pmatrix} E\delta + E\xi_E \\ I\delta + Ir_I - E\eta_I\xi_E \\ U\delta + Ur_U - E\left(1-\eta_I\right)\xi_E \end{pmatrix}.$$

At DFE E_0, the Jacobian matrix of $F(t)$ and $G(t)$ are given as

$$J_F = \begin{pmatrix} 0 & \frac{\rho_S \vartheta_I \chi_S}{\lambda} & \frac{\rho_S \vartheta_U \chi_S}{\mathrm{Y}} \\ 0 & 0 & 0 \\ 0 & 0 & 0 \end{pmatrix} \text{ and } J_V = \begin{pmatrix} \delta + \xi_E & 0 & 0 \\ -\eta_I \xi_E & \delta + r_I & 0 \\ (\eta_I - 1)\xi_E & 0 & \delta + r_U \end{pmatrix}.$$

$$J_F J_V^{-1} = \begin{pmatrix} \frac{\eta_I \xi_E \rho_S \vartheta_I \chi_S}{\lambda(\delta + r_I)(\delta + \xi_E)} - \frac{(\eta_I - 1)\xi_E \rho_S \vartheta_U \chi_S}{\lambda(\delta + r_U)(\delta + \xi_E)} & \frac{\rho_S \vartheta_I \chi_S}{\lambda(\delta + r_I)} & \frac{\rho_S \vartheta_U \chi_S}{\lambda(\delta + r_U)} \\ 0 & 0 & 0 \\ 0 & 0 & 0 \end{pmatrix}$$

is the next generation matrix and the BR number is

$$R_0 = \frac{\xi_E \rho_S \chi_S \left(\eta_I \vartheta_I (\delta + r_U) + (1 - \eta_I)\vartheta_U (\delta + r_I)\right)}{\lambda(\xi_E + \delta)(\delta + r_I)(\delta + r_U)}. \tag{22}$$

5.2 *Stability of DFE*

Theorem 5.2. The DFE E_0 of the proposed fractional-order COVID-19 model (4) is locally asymptotically stable if $R_0 < 1$ and is unstable if $R_0 > 1$.

Proof. The Jacobian matrix at E_0 is

$$J(E_0) = \begin{pmatrix} -\lambda & 0 & -\frac{\rho_S \vartheta_I \chi_S}{\lambda} & -\frac{\rho_S \vartheta_U \chi_S}{\lambda} & 0 \\ 0 & -\delta - \xi_E & \frac{\rho_S \vartheta_I \chi_S}{\lambda} & \frac{\rho_S \vartheta_U \chi_S}{\lambda} & 0 \\ 0 & \eta_j \xi_E & -\delta - r_I & 0 & 0 \\ 0 & (1 - \eta_j)\xi_E & 0 & -\delta - r_U & 0 \\ 0 & 0 & r_I & r_U & -\delta \end{pmatrix}.$$

Thus, the DFE E_0 is locally asymptotically stable if all the eigenvalues $\Theta_i, i = 1, 2, \cdots, 5,$ of the Jacobian matrix $J(E_0)$ admits

$$|arg(eig(J(E_0)))| = |arg(\Theta_i)| > \frac{\alpha\pi}{2}, i = 1, 2, \cdots, 5. \tag{23}$$

The characteristic equation is

$$(\delta + \Theta)(\lambda + \Theta)(\Theta^3 + A_1\Theta^2 + A_2\Theta + A_3) = 0.$$

This yields $\Theta_1 = -\delta < 0, \Theta_2 = -\lambda < 0,$ and

$$\Theta^3 + A_1\Theta^2 + A_2\Theta + A_3 = 0, \tag{24}$$

where $A_1 = \xi_E + 3\delta + r_I + r_U > 0,$

$$A_2 = \frac{1}{\lambda}(2\delta\lambda\xi_E + \lambda\xi_E r_I + \xi_E\eta_I\rho_s\chi_s(\vartheta_U - \vartheta_I) + \lambda\xi_E r_U - \xi_E\rho_S\chi_S\vartheta_U + 3\delta^2\lambda + 2\delta\lambda r_I + \lambda r_I r_U + 2\delta\lambda r_U > 0,$$
$$A_3 = \frac{1}{\lambda^2(\xi_E+\delta)(\delta+r_I)(\delta+r_U)}(1-R_0).$$

Clearly, $A_1 > 0$, $A_2 > 0$. We have $A_3 > 0$ if $R_0 < 1$. This concludes that DFE point E_0 is stable if $R_0 < 1$.

5.3 *Existence and stability of endemic equilibrium point*

The endemic equilibrium point is $E^* = (S^*, E^*, I^*, U^*, R^*)$, where

$$S^* = \frac{(\xi_E+\delta)(\delta+r_I)(\delta+r_U)}{\xi_E\rho_S\left(\eta_I(\vartheta_I(\delta+r_U)-\vartheta_U(\delta+r_I))+\vartheta_U(\delta+r_I)\right)} = \frac{\chi_S}{\lambda R_0},$$
$$E^* = \frac{\lambda(R_0-1)S^*}{\xi_E+\delta},$$
$$I^* = \frac{\eta_I\xi_E\lambda(R_0-1)S^*}{(r_I+\delta)(\xi_E+\delta)},$$
$$U^* = \frac{\xi_E(1-\eta_I)\lambda(R_0-1)S^*}{(r_U+\delta)(\xi_E+\delta)},$$
$$R^* = \frac{(\eta_I\xi_E + r_U\xi_E(1-\eta_I))\lambda(R_0-1)S^*}{(r_U+\delta)(\xi_E+\delta)}.$$

Endemic equilibrium point exists if $R_0 > 1$.

Theorem 5.3. The endemic equilibrium E^* of the proposed fractional-order model (4) is locally asymptotically stable if $R_0 > 1$ and unstable otherwise.

Proof. The Jacobian matrix at E^* is

$$J(E^*) = \begin{pmatrix} -\lambda R_0 & 0 & -\frac{\rho_S\vartheta_I\chi_S}{\lambda R_0} & -\frac{\rho_S\vartheta_U\chi_S}{\lambda R_0} & 0 \\ (R_0-1)\lambda & -\delta-\xi_E & \frac{\rho_S\vartheta_I\chi_S}{\lambda R_0} & \frac{\rho_S\vartheta_U\chi_S}{\lambda R_0} & 0 \\ 0 & \eta_I\xi_E & -\delta-r_I & 0 & 0 \\ 0 & (1-\eta_I)\xi_E & 0 & -\delta-r_U & 0 \\ 0 & 0 & r_I & r_U & -\delta \end{pmatrix}.$$

The characteristic polynomial is

$$(\Theta+\delta)(\Theta^4 + B_1\Theta^3 + B_2\Theta^2 + B_3\Theta^+ B_4) = 0, \tag{25}$$

where

$$B_1 = \xi_E + 3\delta + r_I + \lambda + r_U + \lambda(R_0-1),$$
$$B_2 = 2\delta\xi_E + \xi_E r_I + \lambda\xi_E + \xi_E r_U + \lambda(R_0-1)\xi_E + 3\delta^2 + 3\delta\lambda + 2\delta r_I + \lambda r_I + \lambda(R_0-1)r_I + r_I r_U$$
$$+ \lambda(R_0-1)r_U + 2\delta r_U + \lambda r_U + 3\delta\lambda(R_0-1) - \frac{\xi_E\rho_s\chi_s\left(\eta_j(\vartheta_I-\vartheta_U)+\vartheta_U\right)}{\lambda R_0},$$

$$B_3 = \delta^2\xi_E + 2\delta\lambda\xi_E + \delta\xi_E r_I + \lambda\xi_E r_I + \lambda(R_0-1)\xi_E r_I + \xi_a r_I r_U + \lambda(R_0-1)\xi_E r_U + \delta\xi_E r_U$$
$$+ \lambda\xi_E r_U + 2\delta\lambda(R_0-1)\xi_E + \delta^3 + 3\delta^2\lambda + \delta^2 r_I + 2\delta\lambda r_I + 2\delta\lambda(R_0-1)r_I + \lambda(R_0-1)r_I r_U$$
$$+ \delta r_I r_U + \lambda r_I r_U + 2\delta\lambda(R_0-1)r_U + \delta^2 r_U + 2\delta\lambda r_U + 3\delta^2\lambda(R_0-1)$$
$$- \frac{\xi_E\rho_s\chi_s\left(\eta_j\left(\vartheta_I(\delta+\lambda+r_U) - \vartheta_U(\delta+r_I+\lambda)\right) + \vartheta_U(\delta+r_I+\lambda)\right)}{\lambda R_0},$$

$$B_4 = \delta^2\lambda\xi_E + \delta\lambda\xi_E r_I + \delta\lambda(R_0-1)\xi_E r_I + \lambda(R_0-1)\xi_E r_I r_U + \lambda\xi_E r_I r_U + \delta\lambda(R_0-1)\xi_E r_U$$
$$+ \delta\lambda\xi_E r_U + \delta^2\lambda(R_0-1)\xi_E + \delta^3\lambda + \delta^2\lambda r_I + \delta^2\lambda(R_0-1)r_I + \delta\lambda(R_0-1)r_I r_U$$
$$+ \delta\lambda r_I r_U + \delta^2\lambda(R_0-1)r_U + \delta^2\lambda r_U + \delta^3\lambda(R_0-1)$$
$$- \frac{\xi_E\rho_s\chi_s\left(\eta_j\left(\tau_j(\delta+r_U) - \vartheta_U(\delta+r_I)\right) + \vartheta_U(\delta+r_I)\right)}{R_0}.$$

By Lemma 5.1, endemic equilibrium point is stable if $R_0 > 1$.

5.4 *Global stability*

Here, we discussed the global asymptotic stability analysis.

Theorem 5.4. The DFE point E_0 is globally asymptotically stable if $Q > 0$, where

$$Q = \left(2\delta(\gamma_1+\theta_1) - \frac{\chi_S\rho}{\lambda}(\vartheta_I\gamma_2 + \vartheta_U\theta_2)\right).$$

Proof. To analyze the global stability of DFE point, we define a positive definite function [52]:

$$X(S,E,I,U,R) = \left(S - \bar{S} - \bar{S}ln\left(\frac{S}{\bar{S}}\right)\right) + E + I + U + R.$$
$$D_t^\alpha X(S,E,I,U,R) \le \left(1 - \frac{\bar{S}}{S}\right)D_t^\alpha S + D_t^\alpha E + D_t^\alpha I + D_t^\alpha U + D_t^\alpha R$$
$$= \left(\frac{S-\bar{S}}{S}\right)(\chi_S - \rho_S S(\vartheta_I I + \vartheta_U U) - \lambda S) + \rho_S S(\vartheta_I I + \vartheta_U U) - \xi_E E - \delta E$$
$$+ \eta_I\xi_E E - r_I I - \delta I + \xi_E(1-\eta_I)E - r_U U - \delta U + r_I I + r_U U - \delta R$$
$$= \left(\frac{S-\bar{S}}{S}\right)(-\lambda(S-\bar{S}) - \rho_S S(\vartheta_I I + \vartheta_U U)) + \rho_S S(\vartheta_I I + \vartheta_U U)$$
$$- \delta(E + I + U + R).$$

Let $\psi_1 < S < \psi_2, \gamma_1 < E, I < \gamma_2$ and $\theta_1 < U, R < \theta_2$.

Then,

$$D_t^\alpha X \le -\frac{\lambda}{\psi_2}(S-\bar{S})^2 - \left(2\delta(\gamma_1+\theta_1) - \frac{\chi_S\rho}{\lambda}(\vartheta_I\gamma_2 + \vartheta_U\theta_2)\right)$$
$$= -\frac{\lambda}{\psi_2}(S-\bar{S})^2 - Q,$$

where

$$Q = 2\delta(\gamma_1 + \theta_1) - \frac{\chi_S \rho}{\lambda}(\vartheta_I \gamma_2 + \vartheta_U \theta_2).$$

Therefore, $D_t^{\alpha} X \le 0$ if $Q > 0$.

5.5 *Sensitivity analysis of R_0*

Here, we have analyzed the sensitivity of the BR number by evaluating the first derivative of BR number with respect to various parameters

$$\frac{\partial R_0}{\partial \rho_S} = \frac{\xi_E \chi_S \left(\eta_I \vartheta_I (\delta + r_U) + (1-\eta_I)\vartheta_U (\delta + r_I)\right)}{\lambda (\xi_E + \delta)(\delta + r_I)(\delta + r_U)},$$

$$\frac{\partial R_0}{\partial \chi_S} = \frac{\xi_E \rho_S \left(\eta_I \vartheta_I (\delta + r_U) + (1-\eta_I)\vartheta_U (\delta + r_I)\right)}{\lambda (\xi_E + \delta)(\delta + r_I)(\delta + r_U)},$$

$$\frac{\partial R_0}{\partial \xi_E} = \frac{\chi_S \rho_S \left(\eta_I \vartheta_I (\delta + r_U) + (1-\eta_I)\vartheta_U (\delta + r_I)\right)}{\lambda (\xi_E + \delta)(\delta + r_I)(\delta + r_U)},$$

$$\frac{\partial R_0}{\partial \vartheta_I} = \frac{\xi_E \eta_I \rho_S \chi_S}{\lambda (\xi_E + \delta)(\delta + r_I)},$$

$$\frac{\partial R_0}{\partial \vartheta_U} = \frac{\xi_E (1-\eta_I) \rho_S \chi_S}{\lambda (\xi_E + \delta)(\delta + r_U)},$$

$$\frac{\partial R_0}{\partial \eta_I} = \frac{\xi_E \rho_S \chi_S \left(\vartheta_I (\delta + r_U) - \vartheta_U (\delta + r_I)\right)}{\lambda (\xi_E + \delta)(\delta + r_I)(\delta + r_U)},$$

$$\frac{\partial R_0}{\partial \delta} = -\frac{\xi_E \rho_S \chi_S \left((1-\eta_I)\vartheta_U (\delta + r_I)^2 (\xi_E + 2\delta + r_U) + \eta_I \vartheta_I (\delta + r_U)^2 (\xi_E + 2\delta + r_I)\right)}{\lambda (\xi_E + \delta)^2 (\delta + r_I)^2 (\delta + r_U)^2},$$

$$\frac{\partial R_0}{\partial r_I} = -\frac{\xi_E \eta_I \vartheta_I \rho_S \chi_S}{\lambda (\xi_E + \delta)(\delta + r_I)^2},$$

$$\frac{\partial R_0}{\partial r_U} = -\frac{\xi_E (1-\eta_I) \rho_S \chi_S \vartheta_U}{\lambda (\xi_E + \delta)(\delta + r_U)^2},$$

$$\frac{\partial R_0}{\partial \lambda} = -\frac{\xi_E \rho_S \chi_S \left(\eta_I \vartheta_I (\delta + r_U) + (1-\eta_I)\vartheta_U (\delta + r_I)\right)}{\lambda^2 (\xi_E + \delta)(\delta + r_I)(\delta + r_U)}.$$

From the above computation, we observe that $\frac{\partial R_0}{\partial \vartheta_I} > 0$ and $\frac{\partial R_0}{\partial r_I} < 0$. If the rate η_I at which exposed population progress towards infected population is less than 1, then

$$\frac{\partial R_0}{\partial \rho_S} > 0, \frac{\partial R_0}{\partial \chi_S} > 0, \frac{\partial R_0}{\partial \xi_E} > 0, \frac{\partial R_0}{\partial \vartheta_U} > 0, \frac{\partial R_0}{\partial \delta} > 0, \frac{\partial R_0}{\partial r_U} < 0, \frac{\partial R_0}{\partial \lambda} < 0.$$

Sensitivity of R_0 cannot be determined based on its derivative with respect to η_I. Sensitivity analysis of the BR number indicates that by controlling the contact rate and transmission rate, and by improving the recovery rate and vaccination rate the disease can be controlled from being endemic.

6. Numerical method

In this section, we have presented the numerical method employed to solve the COVID-19 vaccination model (4). We use the generalized ABM technique [51] to solve the system (4). Consider the nonlinear equation below:

$$D_t^{\alpha} x(t) = f(t, x(t)), \quad 0 \le t \le T,$$
$$x^{(m)}(0) = x_0^{(m)}, \quad m = 0,1,2,3,...,\nu...,\nu = [\alpha].$$

The corresponding Volterra integral equation may be written as

$$x(t) = \sum_{m=0}^{\nu-1} x_0^{(m)} \frac{t^m}{m!} + \frac{1}{\Gamma(\alpha)} \int_0^t (t-s)^{\alpha-1} f(s, x(s)) ds. \tag{26}$$

In order to integrate (26), the ABM scheme was employed in [47, 48, 50, 57]. Set $h = \frac{T}{N}, t_n = nh, n = 0,1,2,..., N \in \mathbb{Z}^+$. Now, by (4) we have

$$\begin{aligned}
S_{n+1} &= S_0 + \frac{h^{\alpha}}{\Gamma(\alpha+2)} \Big(\chi_S - \rho_S S_{n+1}^P (\vartheta_I I_{n+1}^P + \vartheta_U U_{n+1}^P) - \lambda S_{n+1}^P + \sum_{i=0}^{n} a_{i,n+1} \Big(\chi_S - \rho_S S_i (\vartheta_I I_i + \vartheta_U U_i) - \lambda S_i \Big) \Big), \\
E_{n+1} &= E_0 + \frac{h^{\alpha}}{\Gamma(\alpha+2)} \Big(\rho_S S_{n+1}^P (\vartheta_I I_{n+1}^P + \vartheta_U U_{n+1}^P) - \xi_E E_{n+1}^P - \delta E_{n+1}^P \\
&\quad + \sum_{i=0}^{n} a_{i,n+1} \Big(\rho_S S_i (\vartheta_I I_i + \vartheta_U U_i) - \xi_E E_i - \delta E_i \Big) \Big), \\
I_{n+1} &= I_0 + \frac{h^{\alpha}}{\Gamma(\alpha+2)} \Big(\eta_I \xi_E E_{n+1}^P - r_I I_{n+1}^P - \delta I_{n+1}^P + \sum_{i=0}^{n} a_{i,n+1} [\eta_I \xi_E E_i - r_I I_i - \delta I_i] \Big), \\
U_{n+1} &= U_0 + \frac{h^{\alpha}}{\Gamma(\alpha+2)} \Big(\xi_E (1-\eta_I) E_{n+1}^P - r_U U_{n+1}^P - \delta U_{n+1}^P \\
&\quad + \sum_{i=0}^{n} a_{i,n+1} \Big(\xi_E (1-\eta_I) E_i - r_U U_i - \delta U_i \Big) \Big), \\
R_{n+1} &= R_0 + \frac{h^{\alpha}}{\Gamma(\alpha+2)} \Big(r_I I_{n+1}^P + r_U U_{n+1}^P - \delta R_{n+1}^P + \sum_{i=0}^{n} a_{i,n+1} \Big(r_I I_i + r_U U_i - \delta R_i \Big) \Big), \\
V_{n+1} &= V_0 + \frac{1-\alpha}{\mathcal{P}(\alpha)} \Big(\lambda S_{n+1} \Big) + \frac{\alpha h^{\alpha}}{\mathcal{P}(\alpha)\Gamma(\alpha+2)} \Big(\lambda S_{n+1}^P + \sum_{i=0}^{n} a_{i,n+1} \Big(\lambda S_i \Big) \Big),
\end{aligned}$$

where

$$\begin{aligned}
S_{n+1}^P &= S_0 + \frac{h^{\alpha}}{\Gamma(\alpha+1)} \sum_{i=0}^{n} b_{i,n+1} \Big(\chi_S - \rho_S S_i (\vartheta_I I_i + \vartheta_U U_i) - \lambda S_i \Big), \\
E_{n+1}^P &= E_0 + \frac{h^{\alpha}}{\Gamma(\alpha+1)} \sum_{i=0}^{n} b_{i,n+1} \Big(\rho_S S_i (\vartheta_I I_i + \vartheta_U U_i) - \xi_E E_i - \delta E_i \Big), \\
I_{n+1}^P &= I_0 + \frac{h^{\alpha}}{\Gamma(\alpha+1)} \sum_{i=0}^{n} b_{i,n+1} \Big(\eta_I \xi_E E_i - r_I I_i - \delta I_i \Big), \\
U_{n+1}^P &= U_0 + \frac{h^{\alpha}}{\Gamma(\alpha+1)} \sum_{i=0}^{n} b_{i,n+1} \Big(\xi_E (1-\eta_I) E_i - r_U U_i - \delta U_i \Big), \\
R_{n+1}^P &= R_0 + \frac{h^{\alpha}}{\Gamma(\alpha+1)} \sum_{i=0}^{n} b_{i,n+1} \Big(r_I I_i + r_U U_i - \delta R_i \Big), \\
V_{n+1}^P &= V_0 + \frac{h^{\alpha}}{\Gamma(\alpha+1)} \sum_{i=0}^{n} b_{i,n+1} \Big(\lambda S_i \Big),
\end{aligned} \tag{27}$$

in which

$$a_{i,n+1} = \begin{cases} n^{\alpha+1} - (n-\alpha)(n+1)^{\alpha}, & i = 0, \\ (n-i+2)^{\alpha+1} + (n-i)^{\alpha+1} - 2(n-i+1)^{\alpha+1}, & 1 \le i \le n, \\ 1, & i = n+1, \end{cases}$$

and $b_{i,n+1} = (n-i+1)^{\alpha} - (n-i)^{\alpha}, \quad 0 \le i \le n.$

7. Numerical simulation

The numerical simulation of the fractional COVID-19 model (4) using real-world data is discussed in this section. According to WHO report, the total population of the world as of April 21, 2021 was N = 7,845,261,000 ≅ 7.9 × 10^9, and the birth rate for the world in 2021 was 17.873 births per 1,000 people. Hence, for every day, we have $\chi_S = \frac{n \times N}{365} = 384159.86$. For the simulation, we used the fractional predictor-corrector method, Mathematica software, and WHO COVID-19 details. The following is a list of global COVID-19 cases as of April 21, 2021: Total confirmed cases: 143,123,631; total deaths: 3,045,018; total recovery cases: 82,117,879; total population fully vaccinated: 207,978,809. We have considered the initial data as of April 21, 2021:

$$S_0(t) = 7045261000, E_0(t) = 0.2873 \times 10^9, I_0(t) = 0.1432 \times 10^9, U_0(t) = 2.875 \times 10^8, R_0(t) = 0.082 \times 10^9,$$

$$V_0(t) = 0.208 \times 10^9, \chi_S = 384159.86, \rho_S = 2.7 \times 10^{-8}, \vartheta_I = 0.01824, \vartheta_U = 0.012, \lambda = 0.028, \xi_E = 0.05965, \delta = 58.28 \times 10^{-6},$$

$$\eta_I = 0.955, r_I = 0.5737, r_U = 0.46.$$

By using the above data and using the fractional predictor-corrector technique discussed in Section 6, we have plotted the graphs of the time history of $S(t)$, $E(t)$, $I(t)$, $U(t)$, $R(t)$, and $V(t)$ for α = 1, 0.9, 0.85, 0.8, and 0.7 to see the effect of FDs on various populations. The estimates show the population in billions. When FDs are added, the behavior of all populations become more realistic, as shown in Figure 2. Even though data on susceptible, exposed, and unreported cases is difficult to come by, we can check the model's validity by looking at global data on infected, recovered, and unreported cases. Figures 2(c), 2(d), and 2(e) reflect approximately the same number when derivative values are fractional-order rather than integer-order. α = 0.8 and α = 0.7 give better representation than other values of α. For comparison, we have referred to the WHO website. As the number of COVID-19 infections in India was at its maximum during April-May 2021, the predicted peak date in India may be considered the global peak. The analysis of model (4) in Figure 2(c) shows that infection is at its peak from May 1, 2021, to May 10, 2021. But seeing the infection trend as of May 10, 2021, looks more realistic, which is reflected at α = 0.7. We can see in Figure 2 that, as the number of days increases, the susceptible, exposed, infected, and unreported population decreases, while the population of recovered and vaccinated individuals increases. It is seen that, due to the influence of vaccination, as the number of days increases, the infection reaches its peak and gradually decreases. In Table 2, using equation (22), we have presented the change in the BR number concerning the real-time worldwide vaccination rate. It is observed that the present model (4) depicts that the vaccination rate has a huge impact on curbing the COVID-19 spread.

Figures 3, 4, 5, and 6 represent the effect of different vaccination rates λ = 0.1172, 0.1436, 0.175, 0.201, and 0.236 on susceptible, exposed, infected, unreported, and recovered populations for α = 1,0.9, 0.8, and 0.7, respectively. From Figure 3 for α = 1, we can see that when the vaccination rate λ is increasing, the susceptible, exposed, infected, and unreported populations are decreasing, and the recovered population is in an increasing trend. Further, from Figures 4, 5, and 6 for α = 0.9, 0.8, and 0.7, respectively, we observed that susceptible, exposed, infected, and unreported populations decline faster than the integer order derivative. Hence, with the increase in vaccination rates, the proposed generalized model helps us capture the reliable and interesting consequences of the projected system.

In Figures 7, 8, and 9, we have intended to figure out the impact of contact on the spread of COVID-19 infection in the presence of the Caputo fractional operator. The fractional operator in the system and its numerical simulation using

the predictor-corrector approach have important implications for examining and forecasting the future of the suggested model.

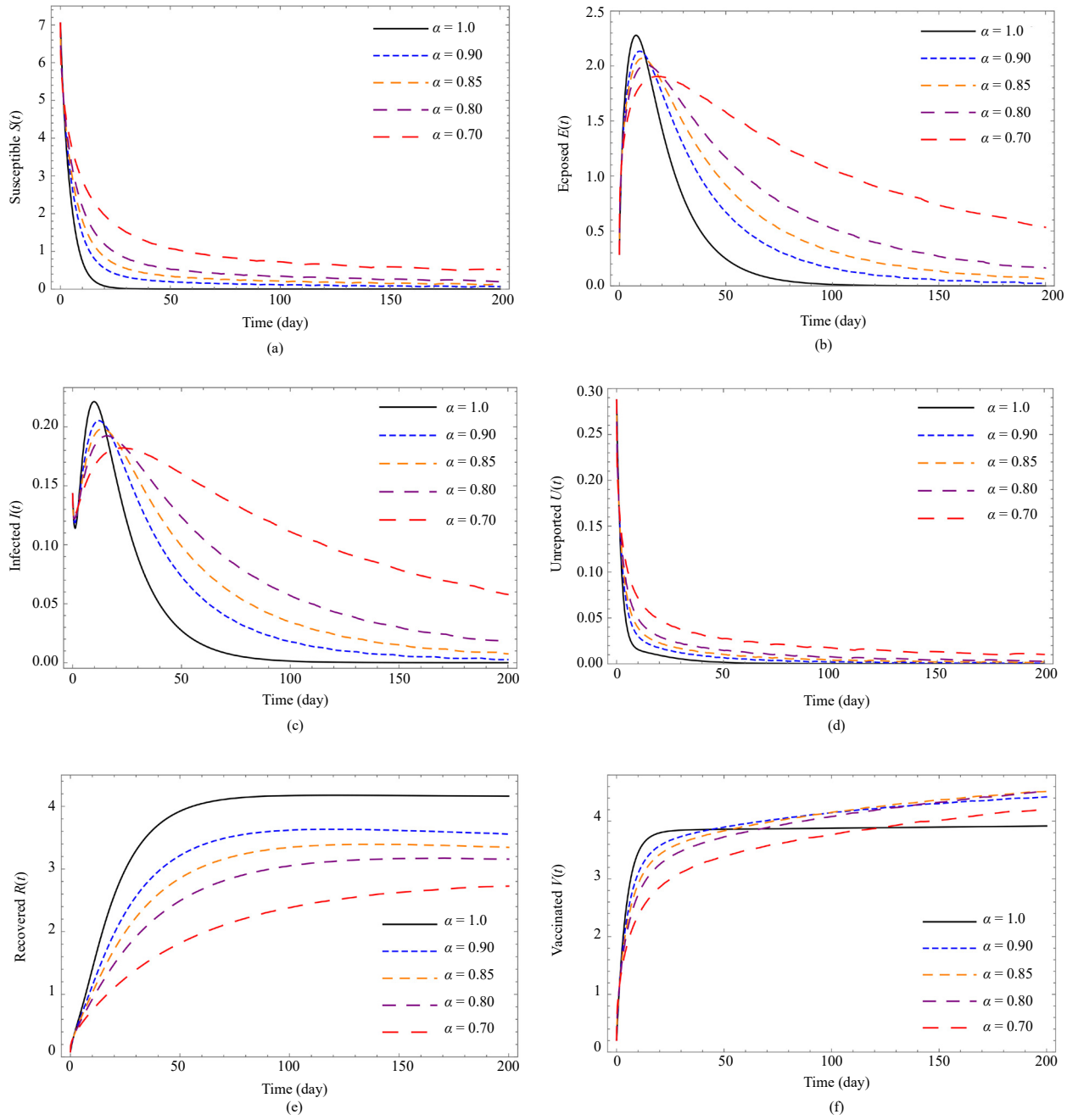

Figure 2. The time history of (a) susceptible, (b) exposed, (c) infected, (d) unreported, (e) recovered, and (f) vaccinated population for different values of α

Table 2. Effect of vaccination rate on BR number. Vaccination rates are collected from [58] as per 2021 data

Date	Rate of vaccination	BR number
Before Jan 19	0.0003	1.08919
Jan 19 to 31	0.001	0.32675
Feb 10	0.003	0.10892
Feb 20	0.005	0.06535
Feb 28	0.007	0.04668
Mar 10	0.009	0.03631
Mar 20	0.013	0.02514
Mar 30	0.016	0.02042
April 21	0.028	0.1167
April 30	0.035	0.00934
May 10	0.042	0.00778
May 20	0.049	0.00667
May 30	0.055	0.00594
June 10	0.063	0.00519
June 20	0.072	0.00454
June 30	0.082	0.00398
July 10	0.093	0.00351
July 20	0.104	0.00314
July 30	0.117	0.00279
Aug 10	0.13	0.00251
Aug 20	0.243	0.00134
Aug 30	0.272	0.00120
Sept 10	0.300	0.00109
Sept 20	0.322	0.00101

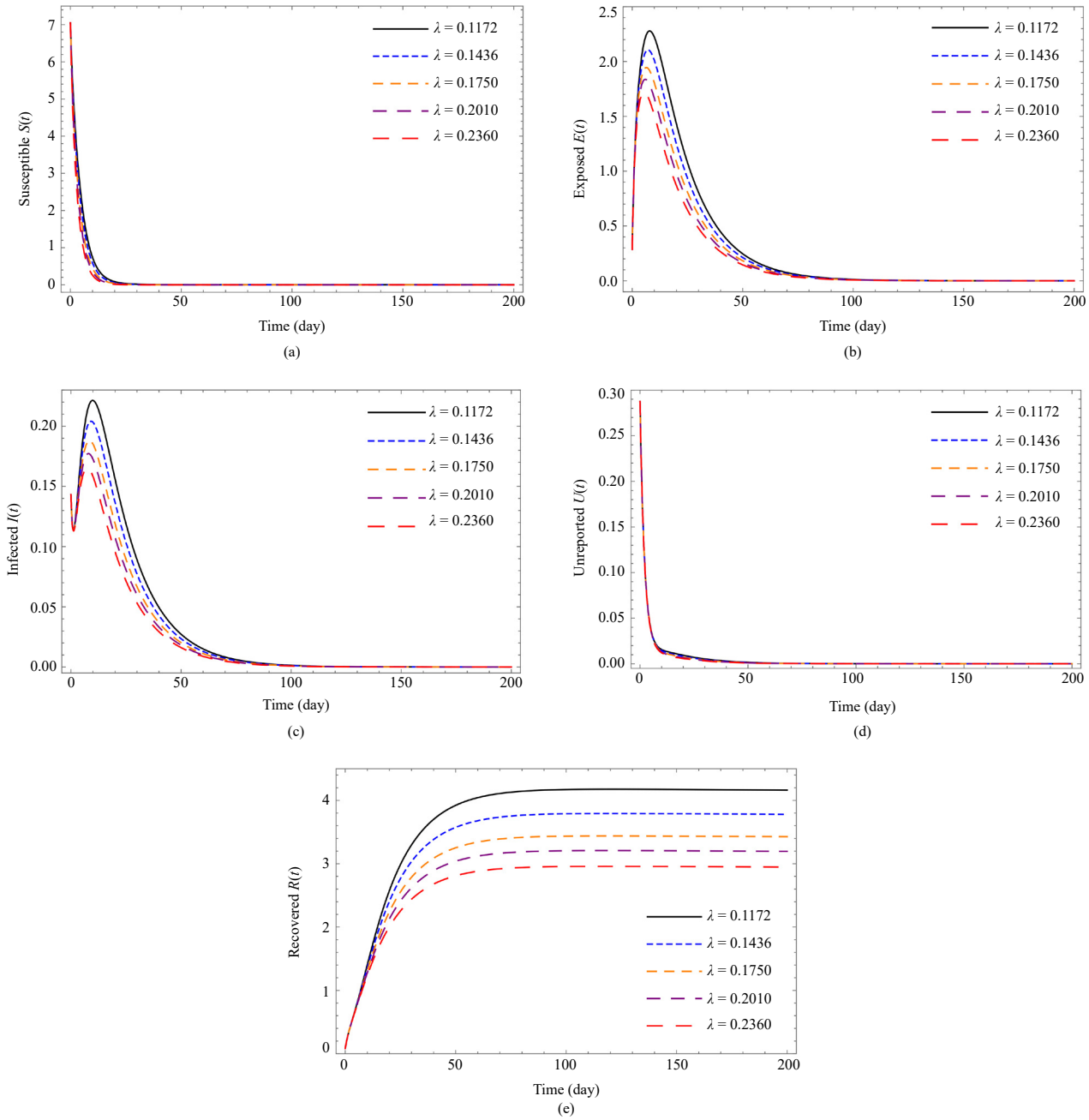

Figure 3. Effect of vaccination on (a) susceptible, (b) exposed, (c) infected, (d) unreported, and (e) recovered population for $\alpha = 1$

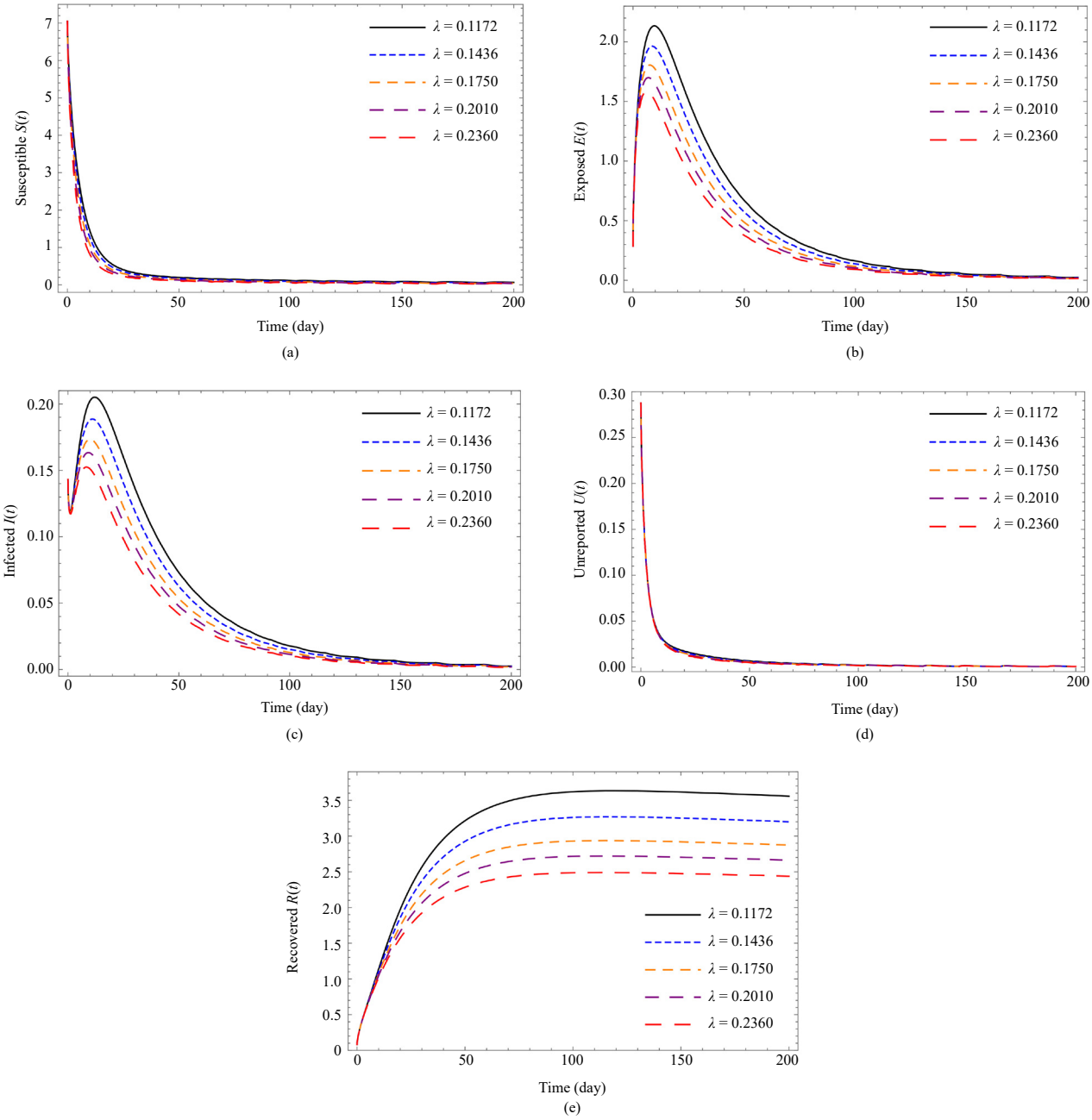

Figure 4. Effect of vaccination on (a) susceptible, (b) exposed, (c) infected, (d) unreported, and (e) recovered population for $\alpha = 0.9$

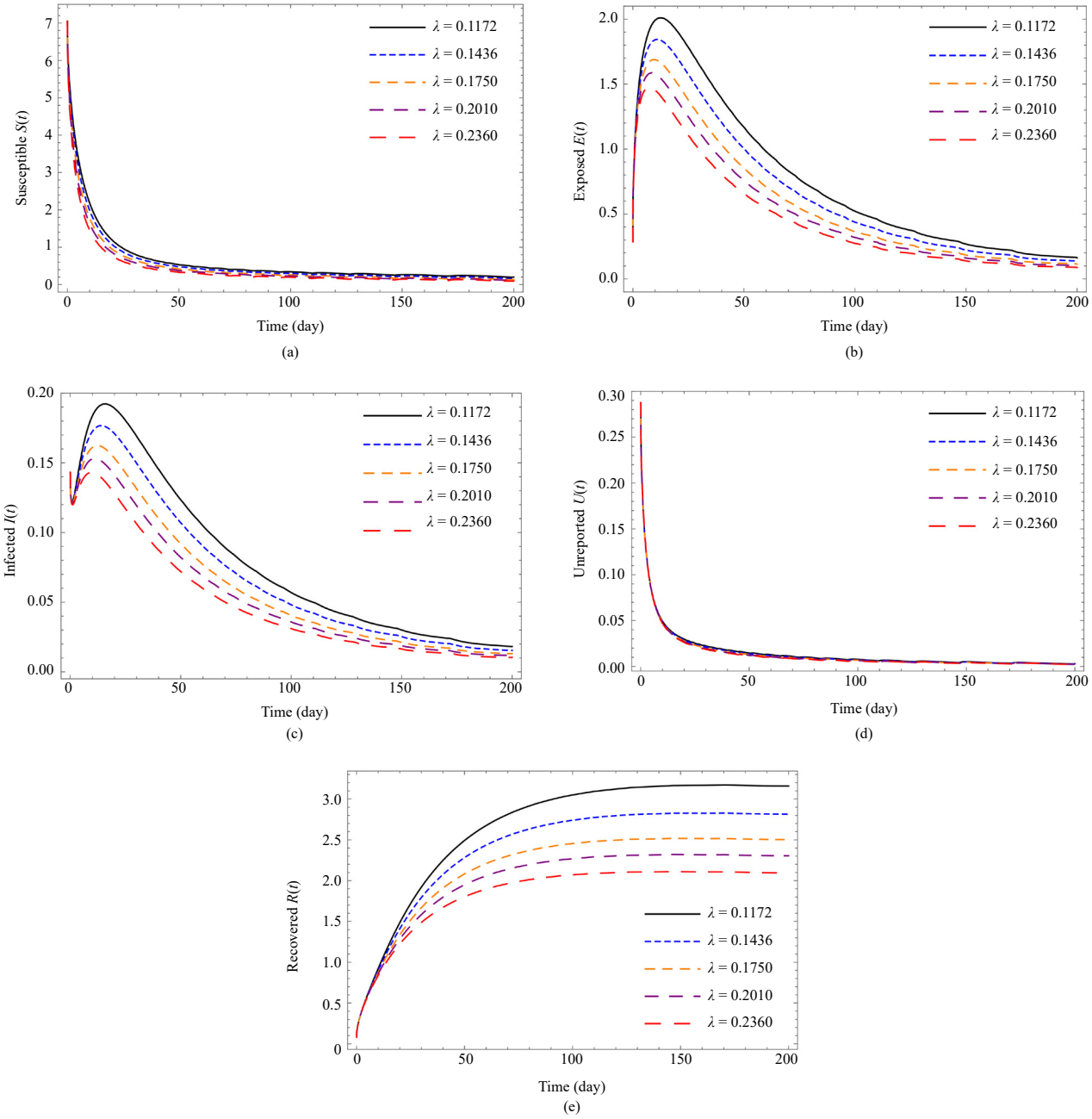

Figure 5. Effect of vaccination on (a) susceptible, (b) exposed, (c) infected, (d) unreported, and (e) recovered population for $\alpha = 0.8$

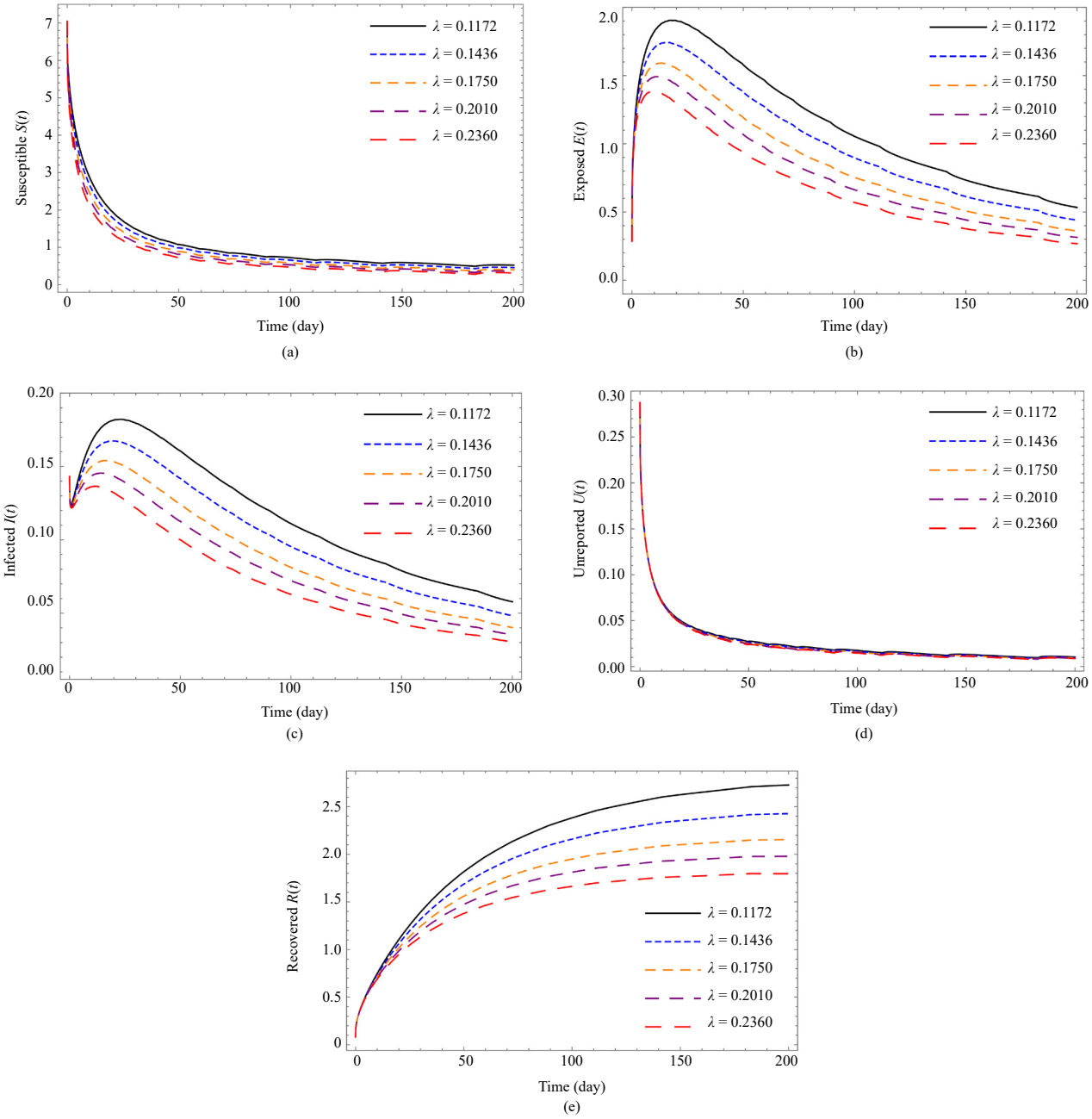

Figure 6. Effect of vaccination on (a) susceptible, (b) exposed, (c) infected, (d) unreported, and (e) recovered population for $\alpha = 0.7$

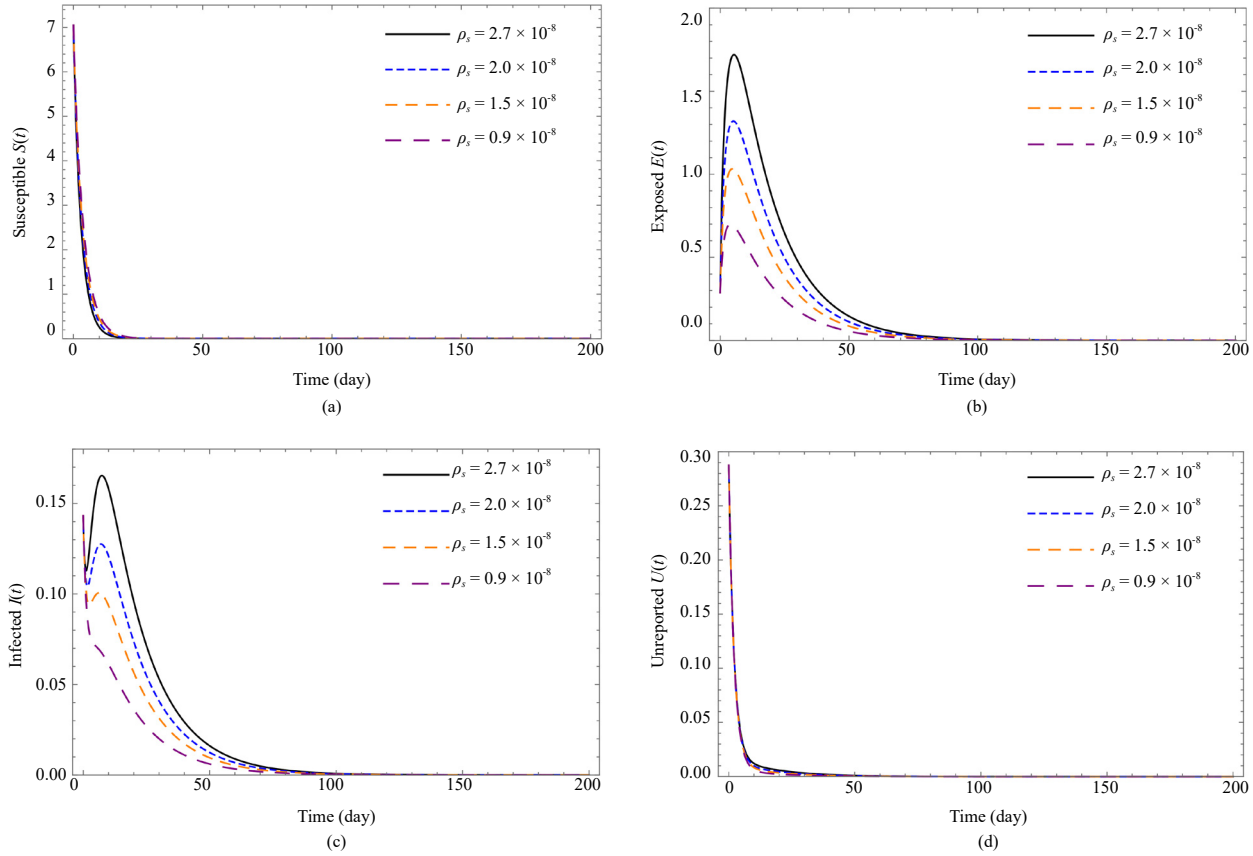

Figure 7. Effect of contact rate on (a) susceptible, (b) exposed, (c) infected, (d) unreported population for $\alpha = 1$

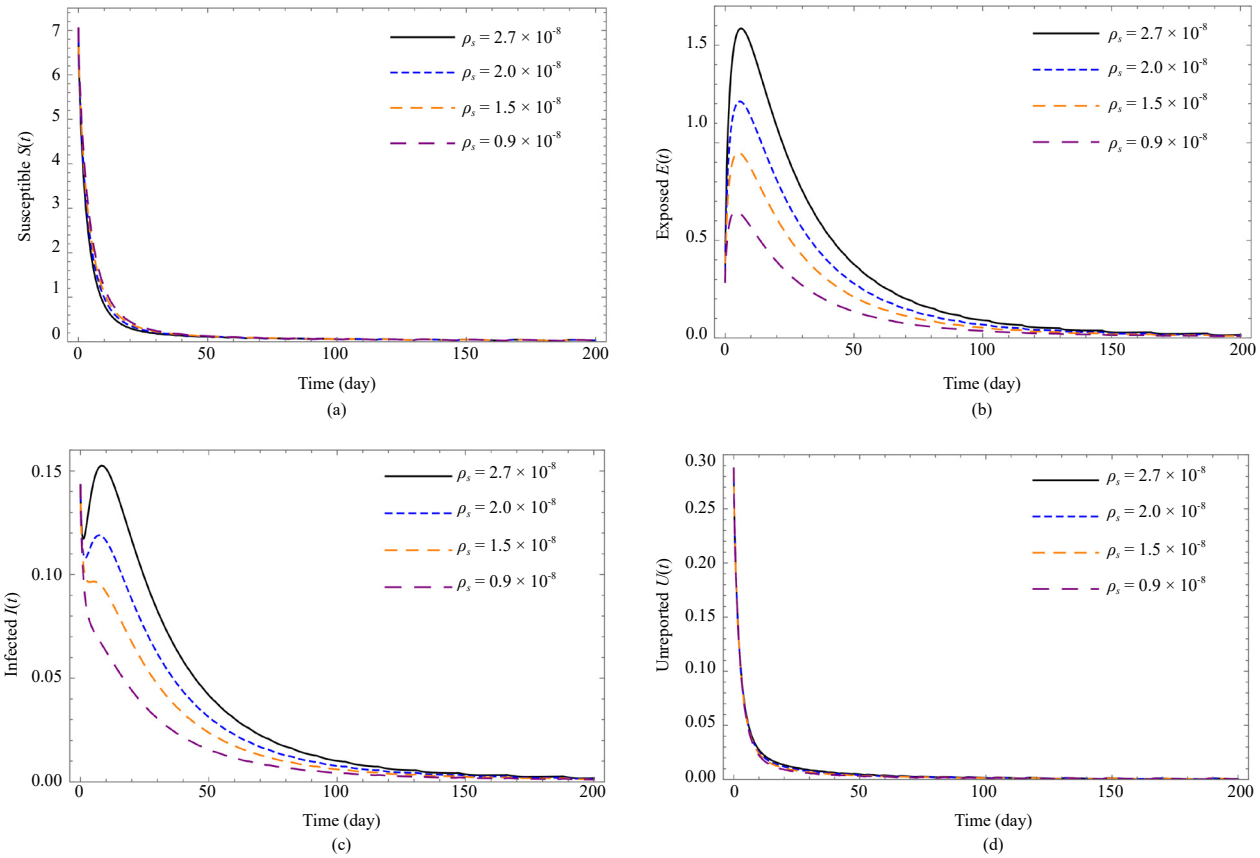

Figure 8. Effect of contact rate on (a) susceptible, (b) exposed, (c) infected, and (d) unreported population for $\alpha = 0.9$

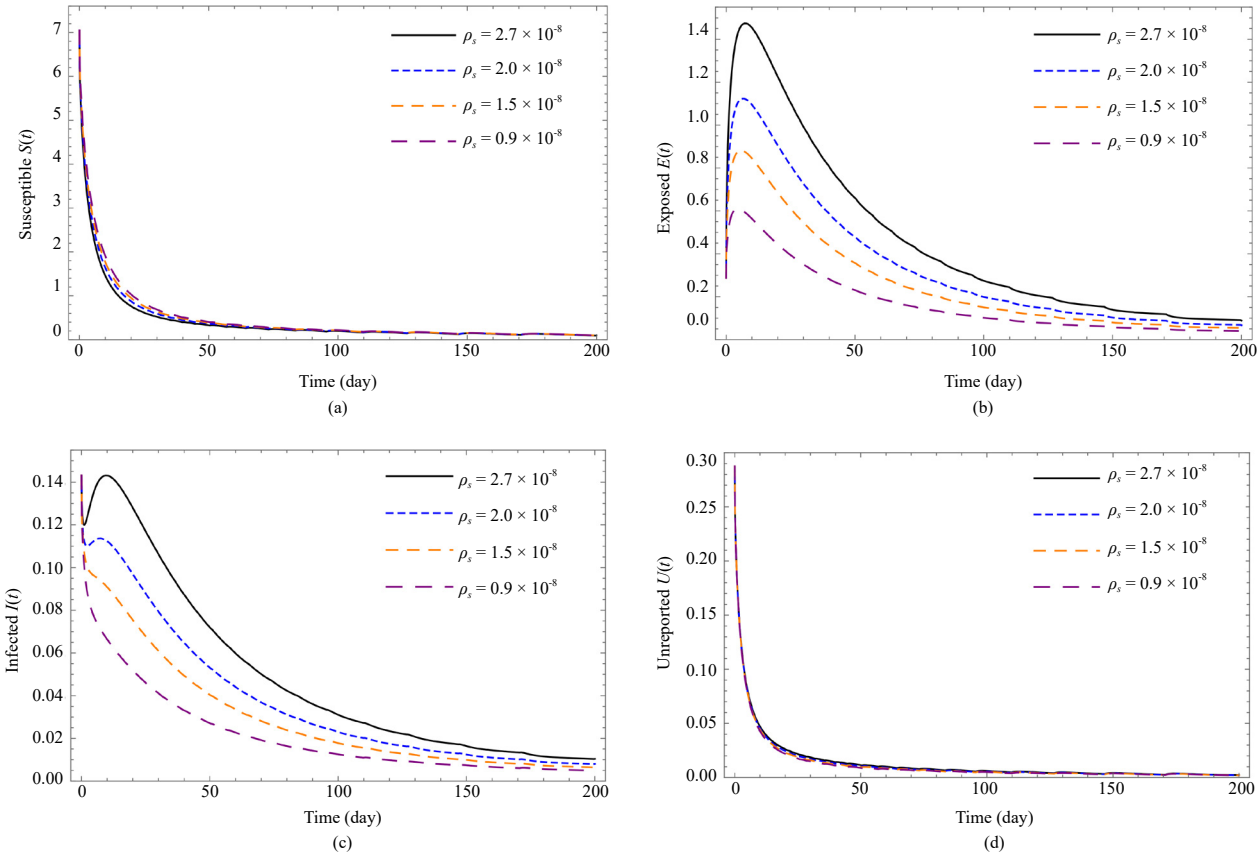

Figure 9. Effect of contact rate on (a) susceptible, (b) exposed, (c) infected, and (d) unreported population for $\alpha = 0.8$

8. Conclusion

The main contribution of this study is the analysis of a mathematical model for propagating the COVID-19 disease in the presence of a vaccination drive in the frame of the Caputo fractional-order derivative. We studied the existence and uniqueness of the solutions using fixed point theory. The BR number R_0 was calculated using the next-generation matrix approach, and it acts as a threshold parameter in disease transmission, determining whether the disease continues or disappears from the population. The existence of an endemic equilibrium point has been investigated. For the projected fractional-order system, the local asymptotic stability conditions of the DFE and endemic equilibrium points have been discussed in terms of BR number, and it has been established that the disease-free equilibrium point is stable if $R_0 < 1$, and the endemic equilibrium point is stable if $R_0 > 1$. We have developed the essential requirements for achieving global stability at equilibrium points by creating the Lyapunov function. In the numerical investigation, we examine the evolution of COVID-19, the effect of vaccination, and the effect of contact rate on its spread by taking 21 April 2021 WHO data as initial data. By evaluating the connection of the Caputo fractional operator with susceptible, exposed, verified, unreported, recovered, and vaccinated populations in the contagion of the novel virus, some important and simulating facts about the COVID-19 vaccination and contact effect are exemplified to understand its evolution and forecast its development globally. In places where vaccination campaigns are being broadly implemented, several apparent trends, such as (a) incidences of serious sickness caused by COVID-19 have decreased as vaccination rates have increased; (b) "breakthrough infections" among fully vaccinated persons are infrequent and usually mild; and (c) cases of major illness resulting in hospitalization or death are now mostly seen in unvaccinated populations, have emerged. This influence of vaccination on curbing the spread of COVID-19 disease is depicted by computing the BR number. A numerical simulation obtained by using the predictor-corrector technique and the computational mathematical tool Mathematica records convincing results. It is observed that plots presented using the fractional-order value of the derivative reveal a more convincing pattern of disease spread than the integer-order derivative. The current study

emphasizes the importance of using a mathematical model when discussing real-world problems and the performance of the fractional operator under consideration. Furthermore, the projected solution procedure for solving the system of fractional differential equations is highly methodical and effective.

This study can be extended by incorporating the socio-economic aspects of COVID-19 infection.

Conflict of interest

The authors declare no competing financial interest.

References

[1] Hunter JC, Nguyen DT, Aden B, Al Bandar Z, Al Dhaheri W, Abu Elkheir K, et al. Transmission of Middle East respiratory syndrome coronavirus infections in healthcare settings, Abu Dhabi. *Emerging Infectious Diseases*. 2016; 22(4): 647-656. Available from: https://doi.org/10.3201/eid2204.151615.

[2] Zhu N, Zhang D, Wang W, Li X, Yang B, Song J, et al. A novel coronavirus from patients with pneumonia in China. *The New England Journal of Medicine*. 2020; 382; 727-733. Available from: https://doi.org/10.1056/NEJMoa2001017.

[3] Gorbalenya AE. The species severe acute respiratory syndrome-related coronavirus: Classifying 2019-nCoV and naming it SARS-CoV-2. *Nature Microbiology*. 2020; 5: 536-544. Available from: https://doi.org/10.1038/s41564-020-0695-z.

[4] Centers for Disease Control and Prevention (CDC). *Symptoms of novel coronavirus (2019-nCoV)*. [Accessed 8th November 2021].

[5] World Health Organization (WHO). *WHO COVID-19 dashboard*. Available from: https://data.who.int/dashboards/covid19/cases [Accessed 8th November 2021].

[6] WHO. *Evaluation of COVID-19 vaccine effectiveness*. Available from: https://www.who.int/publications/i/item/WHO-2019-nCoV-vaccine_effectiveness-measurement-2021.1 [Accessed 17th March 2021].

[7] WHO. *COVID-19 vaccines*. Available from: https://www.who.int/emergencies/diseases/novel-coronavirus-2019/covid-19-vaccines [Accessed 20th November 2021].

[8] Lu S. Timely development of vaccines against SARS-CoV-2. *Emerging Microbes & Infections*. 2020; 9(1): 542-544. Available from: https://doi.org/10.1080/22221751.2020.1737580.

[9] National Institutes of Health (NIH). *NIH clinical trial of investigational vaccine for COVID-19 begins*. Available from: https://www.nih.gov/news-events/news-releases/nih-clinical-trial-investigational-vaccine-covid-19-begins [Accessed 21st November 2021].

[10] Caputo M. Linear models of dissipation whose Q is almost frequency independent-II. *Geophysical Journal International*. 1967; 13(5): 529-539. Available from: https://doi.org/10.1111/j.1365-246X.1967.tb02303.x.

[11] Achar SJ, Baishya C, Kaabar MKA. Dynamics of the worm transmission in wireless sensor network in the framework of fractional derivatives. *Mathematical Methods in the Applied Sciences*. 2022; 45(8): 4278-4294. Available from: https://doi.org/10.1002/mma.8039.

[12] Kilbas AA, Srivastava HM, Trujillo JJ. *Theory and applications of fractional differential equations*. Elsevier; 2006.

[13] Podlubny I. *Fractional differential equations*. Academic Press; 1999.

[14] Ross B. A brief history and exposition of the fundamental theory of fractional calculus. In: *Fractional calculus and its applications.* Berlin, Heidelberg: Springer; 1975. p.1-36.

[15] Caputo M, Fabrizio M. A new definition of fractional derivative without singular kernel. *Progress in Fractional Differentiation and Applications*. 2015; 1(2): 73-85.

[16] Baishya C, Achar SJ, Veeresha P, Prakasha DG. Dynamics of a fractional epidemiological model with disease infection in both the populations. *Chaos: An Interdisciplinary Journal of Nonlinear Science*. 2021; 31(4): 043130. Available from: https://doi.org/10.1063/5.0028905.

[17] Taghvaei A, Georgiou TT, Norton L, Tannenbaum A. Fractional SIR epidemiological models. *Scientific Reports.*

2020; 10: 20882. Available from: https://doi.org/10.1038/s41598-020-77849-7.
[18] Vellappandi M, Kumar P, Govindaraj V. Role of vaccination, the release of competitor snails, chlorination of water, and treatment controls on the transmission of bovine schistosomiasis disease: A mathematical study. *Physica Scripta*. 2022; 97(7): 074006. Available from: https://doi.org/10.1088/1402-4896/ac7421.
[19] Achar SJ, Baishya C, Veeresha P, Akinyemi L. Dynamics of fractional model of biological pest control in tea plants with Beddington-DeAngelis functional response. *Fractal and Fractional*. 2022; 6(1): 1. Available from: https://doi.org/10.3390/fractalfract6010001.
[20] Haq F, Shah K, Rahman G-U, Shahzad M. Numerical analysis of fractional order model of HIV-1 infection of CD4+ T-cells. *Computational Methods for Differential Equations*. 2017; 5(1): 1-11.
[21] Baishya C, Veeresha P. Laguerre polynomial-based operational matrix of integration for solving fractional differential equations with non-singular kernel. *Proceedings of the Royal Society A*. 2021; 477(2253). Available from: https://doi.org/10.1098/rspa.2021.0438.
[22] Baishya C. An operational matrix based on the independence polynomial of a complete bipartite graph for the Caputo fractional derivative. *SeMA Journal*. 2022; 79: 699-717. Available from: https://doi.org/10.1007/s40324-021-00268-9.
[23] Vellappandi M, Kumar P, Govindaraj V. Role of fractional derivatives in the mathematical modeling of the transmission of Chlamydia in the United States from 1989 to 2019. *Nonlinear Dynamics*. 2023; 111: 4915-4929. Available from: https://doi.org/10.1007/s11071-022-08073-3.
[24] Vellappandi M, Kumar P, Govindaraj V, Albalawi W. An optimal control problem for mosaic disease via Caputo fractional derivative. *Alexandria Engineering Journal*. 2022; 61(10): 8027-8037. Available from: https://doi.org/10.1016/j.aej.2022.01.055.
[25] Owolabi KM. Behavioural study of symbiosis dynamics via the Caputo and Atangana-Baleanu fractional derivatives. *Chaos, Solitons & Fractals*. 2019; 122: 89-101. Available from: https://doi.org/10.1016/j.chaos.2019.03.014.
[26] Shah SAA, Khan MA, Farooq M, Ullah S, Alzahrani EO. A fractional order model for Hepatitis B virus with treatment via Atangana-Baleanu derivative. *Physica A: Statistical Mechanics and its Applications*. 2020; 538: 122636. Available from: https://doi.org/10.1016/j.physa.2019.122636.
[27] Koca I. Analysis of rubella disease model with non-local and non-singular fractional derivatives. *An International Journal of Optimization and Control: Theories & Applications*. 2018; 8(1): 17-25. Available from: https://doi.org/10.11121/ijocta.01.2018.00532.
[28] Khan MA. Hammouch Z, Baleanu D. Modeling the dynamics of hepatitis E via the Caputo-Fabrizio derivative. *Mathematical Modelling of Natural Phenomena*. 2019; 14(3): 311. Available from: https://doi.org/10.1051/mmnp/2018074.
[29] Baleanu D, Jajarmi A, Mohammadi H, Rezapour S. A new study on the mathematical modelling of human liver with Caputo-Fabrizio fractional derivative. *Chaos, Solitons & Fractals*. 2020; 134: 109705. Available from: https://doi.org/10.1016/j.chaos.2020.109705.
[30] Kojabad EA, Rezapour S. Approximate solutions of a sum-type fractional integro-differential equation by using Chebyshev and Legendre polynomials. *Advances in Difference Equations.* 2017; 2017: 1-18. Available from: https://doi.org/10.1186/s13662-017-1404-y.
[31] Qureshi S, Memon Z-u-N. Monotonically decreasing behavior of measles epidemic well captured by Atangana-Baleanu-Caputo fractional operator under real measles data of Pakistan. *Chaos, Solitons & Fractals*. 2020; 131: 109478. Available from: https://doi.org/10.1016/j.chaos.2019.109478.
[32] Rajagopal K, Hasanzadeh N, Parastesh F, Hamarash II, Jafari S, Hussain I. A fractional-order model for the novel coronavirus (COVID-19) outbreak. *Nonlinear Dynamics*. 2020; 101(1): 711-718. Available from: https://doi.org/10.1007/s11071-020-05757-6.
[33] Sweilam NH, Al-Mekhlafi SM, Baleanu D. A hybrid stochastic fractional order coronavirus (2019-nCov) mathematical model. *Chaos, Solitons & Fractals*. 2021; 145: 110762. Available from: https://doi.org/10.1016/j.chaos.2021.110762.
[34] Ali A, Alshammari FS, Islam S, Khan MA, Ullah S. Modeling and analysis of the dynamics of novel coronavirus (COVID-19) with Caputo fractional derivative. *Results in Physics*. 2021; 20: 103669. Available from: https://doi.

org/10.1016/j.rinp.2020.103669.
[35] Omar OA, Elbarkouky RA, Ahmed HM. Fractional stochastic models for COVID-19: Case study of Egypt. *Results in Physics*. 2021; 23: 104018. Available from: https://doi.org/10.1016/j.rinp.2021.104018.
[36] Atangana A. Modelling the spread of COVID-19 with new fractal-fractional operators: Can the lockdown save mankind before vaccination? *Chaos, Solitons & Fractals*. 2020; 136: 109860. Available from: https://doi.org/10.1016/j.chaos.2020.109860.
[37] Khan MA, Atangana A. Modeling the dynamics of novel coronavirus (2019-nCov) with fractional derivative. *Alexandria Engineering Journal*. 2020; 59(4): 2379-2389. Available from: https://doi.org/10.1016/j.aej.2020.02.033.
[38] Zhou Y, Ma Z, Brauer F. A discrete epidemic model for SARS transmission and control in China. *Mathematical and Computer Modelling*. 2004; 40(13): 1491-1506. Available from: https://doi.org/10.1016/j.mcm.2005.01.007.
[39] Bahloul MA, Chahid A, Laleg-Kirati T-M. Fractional-order SEIQRDP model for simulating the dynamics of COVID-19 epidemic. *IEEE Open Journal of Engineering in Medicine and Biology*. 2020; 1: 249-256. Available from: https://doi.org/10.1109/OJEMB.2020.3019758.
[40] Ahmad S, Ullah A, Al-Mdallal QM, Khan H, Shah K, Khan A. Fractional order mathematical modeling of COVID-19 transmission. *Chaos, Solitons & Fractals*. 2020; 139: 110256. Available from: https://doi.org/10.1016/j.chaos.2020.110256.
[41] Gao W, Veeresha P, Baskonus HM, Prakasha DG, Kumar P. A new study of unreported cases of 2019-nCOV epidemic outbreaks. *Chaos, Solitons & Fractals*. 2020; 138: 109929. Available from: https://doi.org/10.1016/j.chaos.2020.109929.
[42] Safare KM, Betageri VS, Prakasha DG, Veeresha P, Kumar S. A mathematical analysis of ongoing outbreak COVID-19 in India through nonsingular derivative. *Numerical Methods for Partial Differential Equations*. 2021; 37(2): 1282-1298. Available from: https://doi.org/10.1002/num.22579.
[43] Vellappandi M, Kumar P, Govindaraj V. A case study of 2019-nCoV in Russia using integer and fractional order derivatives. *Mathematical Methods in the Applied Sciences*. 2023; 46(12): 12258-12272. Available from: https://doi.org/10.1002/mma.8736.
[44] Pimenov A, Kelly TC, Korobeinikov A, O'Callaghan MJA, Pokrovskii AV, Rachinskii D. Memory effects in population dynamics: Spread of infectious disease as a case study. *Mathematical Modelling of Natural Phenomena*. 2012; 7(3): 204-226. Available from: https://doi.org/10.1051/mmnp/20127313.
[45] Beisner BE, Haydon D, Cuddington KL. Hysteresis. In: Jørgensen SE, Fath BD. (eds.) *Encyclopedia of ecology*. Elsevier; 2008. p.1930-1935. Available from: https://doi.org/10.1016/B978-008045405-4.00187-7.
[46] Yamana TK, Qiu X, Eltahir EAB. Hysteresis in simulations of malaria transmission. *Advances in Water Resources*. 2017; 108: 416-422. Available from: https://doi.org/10.1016/j.advwatres.2016.10.003.
[47] Diethelm K. An algorithm for the numerical solution of differential equations of fractional order. *Electronic Transactions on Numerical Analysis*. 1997; 5: 1-6.
[48] Diethelm K, Ford NJ. Analysis of fractional differential equations. *Journal of Mathematical Analysis and Applications*. 2002; 265(2): 229-248. Available from: https://doi.org/10.1006/jmaa.2000.7194.
[49] Naik MK, Baishya C, Veeresha P, Baleanu D. Design of a fractional-order atmospheric model via a class of ACT-like chaotic system and its sliding mode chaos control. *Chaos: An Interdisciplinary Journal of Nonlinear Science*. 2023; 33(2): 023129. Available from: https://doi.org/10.1063/5.0130403.
[50] Diethelm K, Ford NJ, Freed AD. A predictor-corrector approach for the numerical solution of fractional differential equations. *Nonlinear Dynamics*. 2002; 29(1): 3-22. Available from: https://doi.org/10.1023/A:1016592219341.
[51] Li C, Tao C. On the fractional Adams method. *Computers & Mathematics with Applications*. 2009; 58(8): 1573-1588. Available from: https://doi.org/10.1016/j.camwa.2009.07.050.
[52] Li H-L, Zhang L, Hu C, Jiang Y-L, Teng Z. Dynamical analysis of a fractional-order predator-prey model incorporating a prey refuge. *Journal of Applied Mathematics and Computing*. 2017; 54(1): 435-449. Available from: https://doi.org/10.1007/s12190-016-1017-8.
[53] Buonomo B. Effects of information-dependent vaccination behavior on coronavirus outbreak: Insights from a SIRI model. *Ricerche di Matematica.* 2020; 69(2): 483-499. Available from: https://doi.org/10.1007/s11587-020-00506-8.

[54] Iboi EA, Ngonghala CN, Gumel AB. Will an imperfect vaccine curtail the COVID-19 pandemic in the U.S.? *Infectious Disease Modelling*. 2020; 5: 510-524. Available from: https://doi.org/10.1016/j.idm.2020.07.006.

[55] Moore S, Hill EM, Tildesley MJ, Dyson L, Keeling MJ. Vaccination and non-pharmaceutical interventions for COVID-19: A mathematical modelling study. *The Lancet Infectious Diseases*. 2021; 21(6): 793-802. Available from: https://doi.org/10.1016/S1473-3099(21)00143-2.

[56] Ahmed E, Elgazzar AS. On fractional order differential equations model for nonlocal epidemics. *Physica A: Statistical Mechanics and its Applications*. 2007; 379(2): 607-614. Available from: https://doi.org/10.1016/j.physa.2007.01.010.

[57] Alkahtani BST, Atangana A, Koca I. Novel analysis of the fractional Zika model using the Adams type predictor-corrector rule for non-singular and non-local fractional operators. *Journal of Nonlinear Sciences and Applications*. 2017; 10(6): 3191-3200. Available from: http://dx.doi.org/10.22436/jnsa.010.06.32.

[58] Our World in Data. *Coronavirus (COVID-19) vaccinations*. Available from: https://ourworldindata.org/covid-vaccinations?country=OWID_WRL [Accessed 22nd November 2021].